4ᵗʰ IFQMS

The 4th International Forum
on Quantum Metrology and Sensing

PROCEEDINGS

Part 1: SE-01, SE-03A, SE-04

December 8th, 2021
Online Conference (Zoom)

QUANTUM
INNOVATION
2021

Organization

The 4th IFQMS (International Forum on Quantum Metrology and Sensing) is held as a Joint Program Session with Quantum Innovation 2021 (December 7-9, 2021).

Date

8 December 2021

Venue

Forum is held on-line.

Language

English

Organized by

Ministry of Education, Culture, Sports, Science and Technology (MEXT)

Committee

Chairperson
Yasuhiko Arakawa (The University of Tokyo)

QI2021 Quantum Sensing Track Chair
Akinari Yokoya (National Institutes for Quantum Science and Technology (QST))

QI2021 Committee Members (Quantum Sensing Track)
Takayuki Iwasaki (Tokyo Institute of Technology)
Tadashi Sakai (Tokyo Institute of Technology)

Contact

Q-LEAP Quantum Metrology and Sensing HQ Secretariat
Email: ifqms@qleap.titech.ac.jp

Program at a Glance

4th International Forum on Quantum Metrology and Sensing

All the times in the program are Japan Standard time (GMT+9)

Dec 8	Session / Presentation	Chairperson / Presenter	Affiliation	Abstract PDF
8:00-10:10	**SE-01. Solid-State Quantum Sensors 1**			
	Chairperson	Takeshi Ohshima	QST	
8:00	Quantum sensing of quantum materials using NV center microscopy	Amir Yacoby	Harvard U	SE-01-01
8:40	Current status and prospects of solid-state quantum sensors for Quantum-LEAP	Mutsuko Hatano	Tokyo Tech	SE-01-02
9:10	Nanoscale vector AC magnetometry with a single nitrogen-vacancy center in diamond	Paola Cappellaro	MIT	SE-01-03
9:40	Planetary magnetic field sensing via electrical readout of quantum centers in SiC	Corey Cochrane	JPL Caltech	SE-01-04
10:10	Break			
10:30-12:10	**SE-02. Quantum Sensors for Life Sciences**			
	Chairperson	Hiroshi Yukawa/Kensuke Osada	QST	
10:30	Production of color centers in nanodiamond	Olga Shenderova	Adamas Nanotechnologie	SE-02-01
11:10	Nitrogen-vacancy centers in nanodiamonds as temperature sensors and immunoassay reporters	Huan-Cheng Chang	Academia Sinica	SE-02-02
11:40	Treatment responses to immune checkpoint inhibitor therapy evaluated by MRI	Shun Kishimoto	NIH	SE-02-03
12:10	Break			
13:10-16:10	**SE-03A. Short Presentations by Young Researchers on SE-01, 04, 06, 07 Topics**			
13:10	SE-A3A-α1 SE-A3A-β1 SE-A3A-γ1 SE-A3A-δ1			
14:30	Break			
14:50	SE-A3A-α2 SE-A3A-β2 SE-A3A-γ2			
13:10-16:10	**SE-03B. Short Presentations by Young Researchers on SE-02, 05 Topics**			
13:10	SE-A3B-01			
14:30	Break			
14:50	SE-A3B-02			
16:10	Break			
17:00-18:40	**SE-04. Solid-State Quantum Sensors 2**			
	Chairperson	Takayuki Iwasaki	Tokyo Tech	
17:00	Quantum sensing enabled by spin qubits in diamond	Fedor Jelezko	Ulm U	SE-04-01
17:40	Programmable quantum simulators based on spins in diamond	Tim Taminiau	TU Delft	SE-04-02
18:10	Development and optimisation of diamond for quantum technologies	Matthew Markham	Element Six	SE-04-03
18:40	Break			
19:00-21:10	**SE-05. Quantum Sensors and Quantum Life Sciences**			
	Chairperson	Ryuji Igarashi	QST	
19:00	Quantum biology: an Introduction	Johnjoe McFadden	U Surrey	SE-05-01
19:40	Avian magnetoreception – a radical sense of direction	Pete J. Hore	U Oxford	SE-05-02
20:10	Surface chemistry of diamond for quantum applications	Anke Krüger	U Wurzburg	SE-05-03
20:40	Diamond-based quantum sensors: technology and applications in physics and biology	Christian Degen	ETH Zurich	SE-05-04
21:10	Closing			

4th IFQMS QUANTUM INNOVATION 2021

Quantum sensing of quantum materials using NV center microscopy

Amir Yacoby

Harvard University

Abstract

The magnetic fields generated by spins and currents provide a unique window into the physics of correlated-electron materials and devices. Proposed only a decade ago, magnetometry based on the electron spin of nitrogen-vacancy (NV) defects in diamond is emerging as a platform that is exceptionally suited for probing condensed matter systems. It can be operated from cryogenic temperatures to above room temperature, has a dynamic range spanning from DC to GHz, and allows sensor-sample distances as small as a few nanometers. As such, NV magnetometry provides access to static and dynamic magnetic and electronic phenomena with nanoscale spatial resolution. While pioneering work focused on proof-of-principle demonstrations of its nanoscale imaging resolution and magnetic field sensitivity, now experiments are starting to probe the correlated-electron physics of magnets and superconductors and to explore the current distributions in low-dimensional materials. In this talk, I will review some of our recent work that uses NV center magnetometry to image skyrmions in thin magnetic films, measure the spin chemical potential in magnetic insulators, and image hydrodynamic electron flow in layered materials. In addition I will describe the use of NV centers in a new scattering platform that uses spin waves as the probing excitation.

SE-01-02

Current status and prospects of solid-state quantum sensors for Quantum-LEAP

Mutsuko Hatano

Tokyo Institute of Technology

Abstract

Solid-state quantum sensors using diamond and SiC are expected to have various applications due to their principle possibilities such as wide-field dynamic range, operating temperature range, and high special resolution down to the atomic level.

In the MEXT Q-LEAP Quantum Solid-state Flagship Project, five companies, five academia, and two national research institutes have teamed up to develop a solid-state quantum sensor from basic science and technologies such as materials and quantum protocols to sensor modules and application prototypes.

In this talk, I would like to introduce the latest research topics of Q-LEAP, such as high precision simultaneous measurement of current and temperature in EV batteries, high-resolution magnetocardiographic imaging of rats, probing into living cells by tip-type NV sensor. In addition, expectations for a future "quantum leap" society based on quantum solid-state sensor technology will be discussed.

This work was supported by MEXT Quantum Leap Flagship Program (MEXT Q-LEAP) Grant Number JPMXS0118067395.

Nanoscale vector AC magnetometry with a single nitrogen-vacancy center in diamond

Paola Cappellaro

Nuclear Science and Engineering, Physics Departments,
Massachusetts Institute of Technology, USA

Abstract

Detection of AC magnetic fields at the nanoscale is critical in applications ranging from fundamental physics to materials science. Isolated nitrogen-vacancy centers in diamond can achieve the desired spatial resolution with high sensitivity. Still, vector AC magnetometry currently relies on using different orientations of an ensemble of sensors, with degraded spatial resolution. Here I will present a novel protocol that exploits a single NV to reconstruct the vectorial components of an AC magnetic field, by tuning a continuous driving to distinct resonance conditions. As an experimental proof-of-principle, I'll show how to map the spatial distribution of an AC field generated by a copper wire on the surface of the diamond.

The proposed protocol combines high sensitivity, broad dynamic range, and sensitivity to both coherent and stochastic signals, with broad applications in condensed matter physics.

4th IFQMS   QUANTUM INNOVATION 2021

Planetary magnetic field sensing via electrical readout of quantum centers in SiC

Corey J. Cochrane

Jet Propulsion Laboratory, California Institute of Technology, United States

Abstract

The most widely used magnetometers for scientific missions to space are fluxgate and optically-pumped atomic-gas instruments due to their high sensitivity, reliability, and proven performance. Fluxgates are simple and robust while the atomic-gas designs are highly accurate and stable. However, it is very difficult to include all of these desired specifications in a single package with adequate size and power constraints for smaller scientific missions that involve cubesats. This opens the door for infusion of next-generation magnetometer technologies. In this work, we report on the development of a silicon carbide magnetometer, promising to be a low complexity, lightweight, low power, and inexpensive alternative to these heritage technologies. It measures magnetic field induced changes in spin dependent recombination (SDR) current within a pn junction. The change in SDR current arises from the interaction of external magnetic fields with the atomic-scale defects in the SiC semiconductor. This change in current can be detected electrically via magnetoresistance caused by zero-field level crossings or low-field electrically-detected magnetic resonance, thereby giving the instrument the ability to self-calibrate, a significant advantage in the remoteness of space. The material properties of SiC, namely radiation and temperature hardness, are also very attractive for space applications in harsh environments.

Quantum Sensing Track : Short Presentations by Young Researchers

SE-03A. Short Presentations by Young Researchers on SE-01, 04, 06, 07 Topics [4th IFQMS]

*Note: Depending on the program, the order of presentations may change within the same group.

All the times in the program are Japan Standard time (GMT+9)

Dec 8 (Wed.)	Session / Presentation	Mentor / Presenter	Affiliation	ID
13:10-14:30	**SE-03A-α1**			
	Mentor	Fedor Jelezko	Ulm U	
	Mentor	Takeshi Ohshima	QST	
	Mentor	Masaki Sekino	U Tokyo	
	Mentor	Takayuki Iwasaki	Tokyo Tech	
	Chair	Motofumi Fushimi	U Tokyo	
	Co-chair	Chikara Shinei	NIMS	
	Exploring NV center formation condition for high Econv and charge-state ratio of NV- and NV0 centers	Chikara Shinei	NIMS	SE-03A-α1-01
	Sensitive atomic magnetometer beyond the standard quantum limit	Kosuke Shibata	Gakushuin U	SE-03A-α1-02*
	Imaging hydrodynamic flow in WTe_2 using cryogenic quantum magnetometry	Uri Vool	Harvard U	SE-03A-α1-03
	Toward on-board magnetoencephalography with wearable magnetometers and active noise canceler	Xinyu Cao	U Tokyo	SE-03A-α1-04
	Continuous-wave temperature sensing using RF-dressed states of nitrogen-vacancy centers in diamond	Hibiki Tabuchi	Keio U	SE-03A-α1-05
	High-quality lead-vacancy centers in diamond by high-pressure and high-temperature annealing	Peng Wang	Tokyo Tech	SE-03A-α1-06
	Magnetocardiography imaging of living rats using NV centers in Diamond	Ryoma Matsuki	Tokyo Tech	SE-03A-α1-07
13:10-14:30	**SE-03A-β1**			
	Mentor	Satoshi Yamasaki	Kanazawa U	
	Mentor	Tokuyuki Teraji	NIMS	
	Mentor	Toshiharu Makino	AIST	
	Mentor	Akimichi Nakazono	YAZAKI	
	Chair	Hiroki Morishita	Kyoto U	
	Co-chair	Moriyoshi Haruyama	AIST	
	Probing correlated phenomena in 2D materials with diamond quantum sensors	Mark Ku	U Delaware	SE-03A-β1-01
	Electroluminescence observation of NV center in diamond lateral p-i-n diode	Moriyoshi Haruyama	AIST	SE-03A-β1-02
	Synthesis of HPHT diamond with controlled nitrogen concentration	Masashi Miyakawa	NIMS	SE-03A-β1-03*
	Formation of diamond film containing perfectly aligned NV center ensembles at a high growth rate by high-power density plasma CVD	Takeyuki Tsuji	Tokyo Tech	SE-03A-β1-04
	High dynamic range current detection using a diamond quantum sensor	Yuta Shigenobu	Tokyo Tech	SE-03A-β1-05
	Vector DC magnetic field sensing with the reference microwave field using nitrogen vacancy centers in diamond	Takuya Isogawa	Keio U	SE-03A-β1-06
	Thermal effects on generation of spin defects in hexagonal boron nitride	Tetta Suzuki	Saitama U, QST	SE-03A-β1-07

Dec 8 (Wed.)	Session / Presentation	Mentor / Presenter	Affiliation	ID
13:10-14:30	**SE-03A-γ1**			
	Mentor	Keiichi Edamatsu	Tohoku U	
	Mentor	Ryosuke Shimizu	UEC	
	Mentor	Hirotaka Terai	NICT	
	Mentor	Ryo Okamoto	Kyoto U	
	Chair	Fumihiro China	NICT	
	Co-chair	Le Bin Ho	Tohoku U	
	Error-disturbance uncertainty relations in faraday measurements	Le Bin Ho	Tohoku U	SE-03A-γ1-01
	Hydrogen annealing effect on silicon optical waveguide	Yixin Wang	Tohoku U	SE-03A-γ1-02
	Wavelength-tunable broadband infrared quantum absorption spectroscopy in the mid-infrared region 2-5 μm	Masaya Arahata	Kyoto U	SE-03A-γ1-03
	Evaluation of superconducting nanowire single photon detectors for mid-infrared wavelengths	Yuki Gama	Kyoto U	SE-03A-γ1-04
	Phase retrieval of joint spectral amplitude	Kemeng Chen	UEC	SE-03A-γ1-05
	Temporal shaping of an entangled-photon wave packet by fourier optical synthesis	Hiroki Oshima	UEC	SE-03A-γ1-06
13:10-14:30	**SE-03A-δ1**			
	Mentor	Takuya Hirano	Gakushuin U	
	Mentor	Takashi Mukaiyama	Osaka U	
	Mentor	Masaki Ando	U Tokyo	
	Mentor	Tadashi Sakai	Tokyo Tech	
	Chair	Kiyotaka Aikawa	Tokyo Tech	
	Co-chair	Satoru Takano	U Tokyo	
	Cryogenic monolithic interferometer for sensing gravity gradient	Satoru Takano	U Tokyo	SE-03A-δ1-01
	Suspension noise measurements of cryogenic torsion pendulums with crystaline fibrfibres	Ching Pin Ooi	U Tokyo	SE-03A-δ1-02
	Angular sensor with a coupled cavity for gravity gradient sensing	Yuka Oshima	U Tokyo	SE-03A-δ1-03
	Towards sensitive accelerometers with levitated single nanoparticles	Kiyotaka Aikawa	Tokyo Tech	SE-03A-δ1-04*
	Interferometric gyroscope using slow and continuous atomic beam	Tomoya Sato	Tokyo Tech	SE-03A-δ1-05*
	Development of a quantum gyroscope based on a signle ion trapping techniques	Ryoichi Saito	Osaka U	SE-03A-δ1-06
	Exponentially enhanced quantum metrology by quenching superradiant light-matter systems beyond the critical point	Karol Gietka	OIST	SE-03A-δ1-07
14:50-16:10	**SE-03A-α2**			
	Mentor	Fedor Jelezko	Ulm U	
	Mentor	Takeshi Ohshima	QST	
	Mentor	Masaki Sekino	U Tokyo	
	Mentor	Takayuki Iwasaki	Tokyo Tech	
	Chair	Chikara Shinei	NIMS	
	Co-chair	Motofumi Fushimi	U Tokyo	
	Three-layered magnetically shielded room for ultrahigh-sensitivity quantum sensing of biomagnetic signals	Motofumi Fushimi	U Tokyo	SE-03A-α2-01
	Super-resolution in nanoscale NMR	Nicolas Staudenmaier	Ulm U	SE-03A-α2-02
	Sensitivity of weight imaging using a hybrid system based on piezoactive magnetic material and diamond quantum sensor	Ryota Kitagawa	Tokyo Tech	SE-03A-α2-03
	Study on electron spin control method for high-sensitivity diamond quantum sensor	Hiroyoshi Tomioka	Tokyo Tech	SE-03A-α2-04
	Optically detected magnetic resonance spectra of silicon vacancies in 4H-SiC with different temperatures	Shu Motoki	QST, Saitama U	SE-03A-α2-05
	High efficiency formation of NV center inside diamond by femtosecond laser	Ryusei Yanoshita	Kyoto U	SE-03A-α2-06

SE-03-A Program 3/3

Dec 8 (Wed.)	Session / Presentation	Mentor / Presenter	Affiliation	ID
14:50-16:10	**SE-03A-β2**			
	Mentor	Satoshi Yamasaki	Kanazawa U	
	Mentor	Tokuyuki Teraji	NIMS	
	Mentor	Toshiharu Makino	AIST	
	Mentor	Akimichi Nakazono	YAZAKI	
	Chair	Moriyoshi Haruyama	AIST	
	Co-chair	Hiroki Morishita	Kyoto U	
	AC magnetic field sensing with ensemble NV centers using electrical detection methods	Hiroki Morishita	Kyoto U	SE-03A-β2-01
	OPuS-MAGNM - miniaturized optically pumped solid state quantum magnetometers for space applications	Hannes Kraus	NASA	SE-03A-β2-02
	Development of phthalocyanine ion beam for creation of multiple NV centers.	Kosuke Kimura	QST, Gunma U	SE-03A-β2-03
	Fabrication of diamond protective film using microwave plasma CVD towards high-quality quantum emitters	Kazuki Hirokawa	Tokyo Tech	SE-03A-β2-04
	A compact quantum sensor head with side excitation of CVD diamond	Yuki Nishio	Tokyo Tech	SE-03A-β2-05
	Hybrid integration of Si3N4 grating structure on diamond NV substrate for efficient photon extraction	Ryota Katsumi	Toyohashi Tech	SE-03A-β2-06
14:50-16:10	**SE-03A-γ2**			
	Mentor	Keiichi Edamatsu	Tohoku U	
	Mentor	Kenichi Nakagawa	UEC	
	Mentor	Ryosuke Shimizu	UEC	
	Mentor	Hirotaka Terai	NICT	
	Chair	Le Bin Ho	Tohoku U	
	Co-chair	Fumihiro China	NICT	
	Superconducting nanostrip single-photon detectors with dielectric multilayer cavities	Fumihiro China	NICT	SE-03A-γ2-01
	Estimation of the quantum efficiency of the up-conversion system based on injection-locked dual oscillators	Masayuki Hojo	Kyoto U	SE-03A-γ2-02
	Selective measurement of biexciton luminescence by photon correlation spectroscopy	Hiroya Seki	UEC	SE-03A-γ2-03
	Towards optical manipulation of gold-nanoparticles for efficient single photon sources	Rui Sun	Tohoku U	SE-03A-γ2-04
	Single photon emission from a quantum-dot-gold-nanostar coupled system on an optical nanofiber	Yining Xuan	Tohoku U	SE-03A-γ2-05
	Focusing constraints on coupling efficiency of collinear type-I degenerated SPDC photon pairs into a single-mode fiber	Nicolas Schwaller	Kyoto U	SE-03A-γ2-06

Note: For the purpose of fostering young researchers, presentations with asterisks (*) are excluded from the short presentation awards.

4th IFQMS

QUANTUM INNOVATION 2021

Exploring NV center formation condition for high E_{conv} and charge-state ratio of NV- and NV0 centers

Chikara Shinei[1], Masashi Miyakawa[1], Shuya Ishii[2], Seiichi Saiki[2], Shinobu Onoda[2],

Kenji Watanabe[1], Takashi Taniguchi[1], Takeshi Ohshima[2] and Tokuyuki Teraji[1]

[1]National Institutes for Materials Science

[2]National Institutes for Quantum Science

SHINEI.Chikara@nims.go.jp

Introduction

Negatively-charged NV center (NV-) is promising color centers for high sensitivity magnetometer due to its long coherence time (~2 ms) and clear Rabi and Ramsey contrast due to spin dependent fluorescence [1]. Weak DC magnetic signal detection such as detection of single-neuron action potential [2], malarial hemozoin [3], biological tissue [4], and paleomagnetic in rocks [5], has been demonstrated using ensemble of NV- center. For the weak DC magnetic signal detection, diamond with [N^T] ranged from 1 to 30 ppm and [NV-] ranged from 0.1 – 4 ppm is empirically suitable. Assuming that the detected volume of diamond is constant, the magnetic sensitivity is proportional to [NV-] which corresponds to the number of elements of the magnetometer. Increasing of [NV-] is the most important for improving the magnetic sensitivity. Generally, the conversion efficiency (E_{conv}) from substitutional nitrogen (N_s^0) to NV- center, [NV-] /[N_s^0], must be increased in order to achieve higher [NV-] [6].

FIG. 1. The relationship [NV-] / [NT] and [NVT] /[NT]

NV centers has also neutral charged state (NV0) which shows no spin dependent fluorescence. Since NV- and NV0 often coexist, fluorescence of NV0 becomes background and reduces fluorescence contrast of NV-. Thus, suppression of NV0 formation while increasing E_{conv} (or [NV-]) is important for improving the sensitivity.

Method and Result

Diamond single crystals used in this study were grown using either HPHT synthesis or CVD method. Substitutional nitrogen concentration was controlled by tuning concentration of Ti in the metal solvent for the former while by changing flow rate of nitrogen gas for the later. After the nitrogen doped diamond growth, an electron beam irradiation was applied with the total fluence of 10^{17}-10^{18} cm^{-2} to create vacancies in the diamond. it was followed by vacuum annealing at 1000℃ for 2h to form NV center in the diamond crystals. The number density ratio of NV- to NV0 is estimated from the intensity ratio of their ZPL. The [NV-] and [N^T] was estimated using EPR method at room temperature. [NV^T] is equal to sum of [NV-] and [NV0].

In FIG. 1, the relationship between [NV-] / [N^T] and [NV^T] / [N^T] measured by EPR and PL is presented. Circles and squares respectively show synthesis method of HPHT and CVD. The color scale indicates substitutional nitrogen concentration [N^T] which was measured before electron beam irradiation process. The solid line shows the case in which [NV-] is equal to [NV^T], indicating all NV center is negative charge state. The rate of increase of [NV-]/[N^T] with respect to [NV^T]/[N^T] becomes smaller when [NV^T]/[N^T] is larger than 20 – 30%. The result indicate that the NV centers were fully negatively charged when [NV^T]/[N^T] was up to about 20%. in our diamond samples. In the presentation, we will discuss physical picture of charge state of NV center depending on [NV^T] / [N^T]: equilibrium equation.

Reference

[1] John F. Barry *et al. Rev. Mod. Phys.* **92**, 015004 (2020).

[2] J. F. Barry *et al.* Proc. Natl. Acad. Sci. U.S.A. **113**, 14133 (2016).

[3] I. Fescenko *et al.* Phys. Rev. Applied **11**, 034029 (2019).

[4] H. C. Davis *et al.* Nat. Commun. **9**, 131 (2018).

[5] D. R. Glenn *et al.* Geochem. Geophys. Geosyst. **18**, 3254 (2017).

[6] J. F. Barry *et al.* Rev. Mod. Phys. **92**, 015004 (2020).
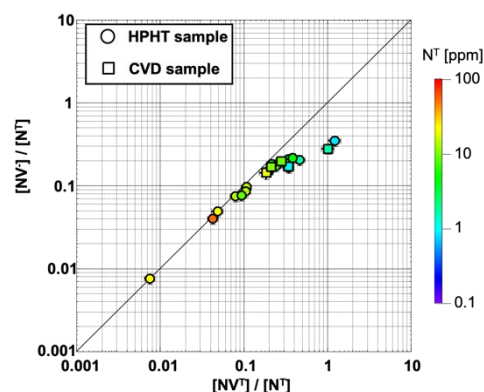
Sensitive atomic magnetometer beyond the standard quantum limit

Kosuke Shibata, Naota Sekiguchi, Aki Torii, Junnosuke Takai, and Takuya Hirano

Department of Physics, Faculty of Science, Gakushuin University

shibata@qo.phys.gakushuin.ac.jp

Introduction

Atoms can be used for sensitive magnetometry. While vapor magnetometers have achieved sub fT Hz$^{-1/2}$ sensitivities [1,2], cold atom gases may work as sensitive and spatially-resolved magnetometers due to small thermal diffusion. Magnetic field sensitivities in the state-of-art atomic magnetometers are limited by the so-called standard quantum limit (SQL), which results from quantum noises. Reduction of the quantum noises below the SQL has attracted attentions as a tool for enhancing performance of a magnetometer.

We have constructed a sensitive magnetometer using a Bose-Einstein condensate (BEC) of rubidium atoms [3]. Our BEC magnetometer sensitivity is already almost limited by quantum noises, consisting of the photon shot noise at detection and atomic spin shot noise. We aim to squeeze both of them to realize a sensitive magnetometer surpassing the classical ones.

Method

We probe a BEC exhibiting the Larmor precession using a two-polarization phase contrast imaging. This imaging setup detects difference in phase shifts of orthogonal circular components of an off-resonant probe at 795 nm, which is proportional to the spin projection along the probe propagation axis and gives the information on the precession phase or a magnetic field at the atom position. The photon shot noise, which naturally appears in this difference detection, can be reduced by adding a squeezed light to the probe. We have successfully generated a squeezed light at the probe wavelength using waveguides and are now constructing a new squeezed light source near the BEC experiment machine. The two-polarization phase contrast detection will introduce spin squeezing on the basis of quantum nondemolition (QND) measurement of an atomic spin variable. We expect that planar squeezed state, which has quantum noise smaller than that in the coherent (classical) spin state in the plane of the Larmor precession [4,5], should be generated in our experiment. The planar squeezed state will improve the magnetic field sensitivity. We have conducted experiments to measure the atomic spin shot noise level and the spin squeezing. I will present on the details of these topics and our recent status.

Reference

[1]I.K. Kominis, T. W. Kornack, J. C. Allred, and M. V. Romalis, *Nature (London)*, 422, 596-599 (2003).

[2]S.-K. Lee, K. L. Sauer, S. J. Seltzer, O. Alem, and M. V. Romalis, *Applied Phys. Lett.*, 89, 214106596-599 (2006).

[3]N. Sekiguchi, K. Shibata, A. Torii, H. Toda, R. Kuramoto, D. Fukuda, and T. Hirano, *Phys. Rev. A*, 104, L041306 (2021).

[4]Q. Y. He, Shi-Guo Peng, P. D. Drummond, and M. D. Reid, *Phys. Rev. A*, 84, 022107 (2011).

[5]G. Puentes, G. Colangelo, R. J. Sewell, and M. W. Mitchell, *New. J. Phys.*, 12, 053007 (2013).

SE-03A-α1-03

Imaging hydrodynamic flow in WTe_2 using cryogenic quantum magnetometry

Uri Vool[1, 2], Assaf Hamo[2], Georgios Varnavides[3, 4, 5], Yaxian Wang[3], Tony X. Zhou[2, 3], Nitesh Kumar6, Yuliya Dovzhenko[2], Ziwei Qiu[2, 3], Christina A. C. Garcia[3], Andrew T. Pierce[2], Johannes Gooth[2, 6, 7], Polina Anikeeva[4, 5], Claudia Felser[3, 6], Prineha Narang[3], and Amir Yacoby[2, 3]

[1]*John Harvard Distinguished Science Fellows Program, Harvard University*

[2]*Department of Physics, Harvard University*

[3]*John A. Paulson School of Engineering and Applied Sciences, Harvard University*

[4]*Department of Materials Science and Engineering, Massachusetts Institute of Technology*

[5]*Research Laboratory of Electronics, Massachusetts Institute of Technology*

[6]*Max-Planck-Institut für Chemische Physik Fester Stoffe, Dresden*

[7]*Institut für Festkörper- und Materialphysik, Technische Universität Dresden*

Hydrodynamic electron flow, where electrons in a conductor flow collectively - akin to a fluid, is a unique signature of strong electron interactions in a material. This effect has been observed in 2D materials, but observations in bulk materials are intriguing as high-carrier density should screen the interactions. In this talk, I will discuss a recent measurement of hydrodynamic flow in the semimetal WTe_2, allowing us to gain insight into the microscopic origin of its electron interactions[1].

We image the spatial profile of the electric current by using a nitrogen-vacancy scanning tip. Using coherent quantum sensing, we obtain magnetic field resolution of ~10nT and spatial resolution of ~100nm. The current pattern we observe differs substantially from the flat profile of a normal metal and indicates correlated flow through the semimetal. The pattern also shows non-monotonic temperature dependence, with hydrodynamic effects peaking at ~20 K.

We compare our results to a model which combines ab initio electron scattering rates and the electronic Boltzmann transport equation. The model shows quantitative agreement with our measurement, allowing us to extract the strength of electron-electron interactions in our material. Furthermore, we conclude that electron interactions are phonon-me diated. This result opens a path for hydrodynamic flow and strong interactions in a variety of new materials.

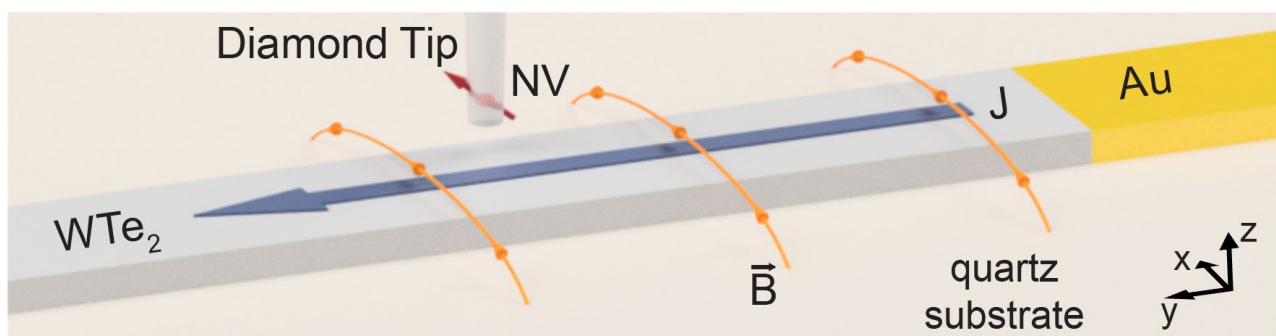
FIG. 1. Measurement technique: imaging local current flow by the effect of its induced magnetic field on a nitrogen-vacancy sensor in a diamond tip.

Reference
[1]U. Vool, A. Hamo, G. Varnavides, Y. Wang *et. al. Nature Physics* 17 1216-1220 (2021)

4th IFQMS

QUANTUM INNOVATION 2021

Toward on-board magnetoencephalography with wearable magnetometers and active noise canceler

Xinyu Cao[1], Zonghao Xin[1], Akihiro Kuwahata[2], Motofumi Fushimi[1], Shinichi Chikaki[1], Kazuhiro Oyama[3], Yuki Anno[3], Teppei Yoshida[3], Takayuki Shibata[3], Yuichiro Shirota[4], Masato Yumoto[4], Hiromasa Sawamura[4], Mutsuko Hatano[5], Takashi Yatsui[6], and Masaki Sekino[1]

[1]*Graduate School of Engineering, The University of Tokyo*

[2]*Graduate School of Engineering, Tohoku University*

[3]*DENSO Corporation*

[4]*Graduate School of Medicine, The University of Tokyo*

[5]*Department of Electrical and Electronic Engineering, Tokyo Institute of Technology*

[6]*Graduate School of Engineering, Toyohashi University of Technology*

caoxinyu@g.ecc.u-tokyo.ac.jp

Introduction

Magnetoencephalography (MEG) is a non-contact biosignal measurement with high temporal and spatial resolution, which has the potential to replace electroencephalogram (EEG) in various application scenarios. This study investigated the feasibility of using wearable magnetometers for applications in on-board MEG. The results provide guidance information for the development of MEG on-board measurement.

Methods

In this study, we proposed the potential application of wearable sensors in on-board MEG measurement, as shown in Figure 1. The steady state visually evoked response (SSVER) signals were measured with superconducting quantum interference devices (SQUIDs), and the signal distribution at potential on-scalp sensor positions were reconstructed with spherical head model [1] and minimum norm estimation (MNE) method [2]. The magnetic fields inside a real car were measured. Noise reduction strategies based on active noise canceler for on-board applications were proposed.
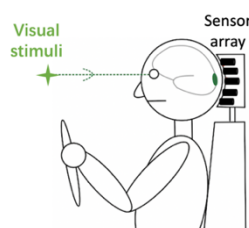

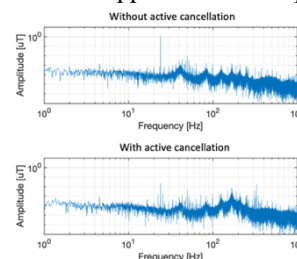FIG. 1. Schematic diagram of on-board MEG measurement based on wearable sensors.

FIG. 2. The FFT of recorded magnetic field without/with active cancellation. Note the change of the peak at 24 Hz.

Results and Discussion

The signal of the simulated wearable sensors is about 3 times that of the SQUID signal in this experiment. After the engine was started, the AC magnetic field inside a gasoline car in an urban environment is about 7 times larger in the vertical direction than in the horizontal direction. The piston movement of the internal combustion engine and the engine fan may be two of the main causes of the magnetic field noise in the car. The highest signal-to-noise ratio of SSVER is -110 dB in this case. A 350 mm 20-turn active cancel coil can attenuate noise by about 28 dB at the target frequency, as shown in Figure 2.

Acknowledgements

References

[1]J. C. Mosher, R. M. Leahy and P. S. Lewis, *IEEE. Trans. Biomed. Eng.*, <u>46</u>, 245-259(1999).

[2]S. Baillet, J. C. Mosher and R. M. Leahy, *IEEE Signal Process Mag*, <u>18</u>, 14-30(2001).

4th IFQMS

QUANTUM INNOVATION 2021

Continuous-Wave Temperature Sensing
using RF-Dressed States of Nitrogen-Vacancy Centers in Diamond

Hibiki Tabuchi[1,2], Yuichiro Matsuzaki[3], Noboru Furuya[1], Yuta Nakano[4], Hideyuki Watanabe[3],

Norio Tokuda[4,5], Norikazu Mizuochi[6], and Junko Ishi-Hayase[1,2]

[1]*School of Fundamental and Technology, Keio University, Japan*

[2]*Center for Spintronics Research Network, Keio University, Japan*

[3]*National Institute of Advanced Industrial Science and Technology (AIST), Japan*

[4]*Graduate School of Natural Science and Technology, Kanazawa University, Japan*

[5]*Nanomaterials Research Institute, Kanazawa University, Japan*

[6]*Institute for Chemical Research, Kyoto University, Japan*

hibiade0914@keio.jp

Introduction

Nowadays, there is a growing need to measure temperature with high sensitivity and special resolution to investigate the properties of cells or nanodevices. A nitrogen-vacancy (NV) center in diamond is a promising candidate to realize a sensitive temperature sensor with a high sensitivity and a special resolution. The temperature sensing using continuous-wave optically-detected magnetic resonance (CW-ODMR) has advantages because this can be simply implemented by continuous applications of a green laser and a microwave field. However, the temperature sensitivity with CW-ODMR is typically worse than that with pulsed-ODMR. Here, we propose a novel way to improve the sensitivity of temperature sensing using CW-ODMR with a quantum state dressed by radio-frequency (RF) fields under the transverse magnetic fields.

Method

Under applying the transverse magnetic fields with respect to the NV axis, the ground electronic spin states of NV center are composed of $|B\rangle=(|+1\rangle+|-1\rangle)/\sqrt{2}$, $|D\rangle=(|+1\rangle-|-1\rangle)/\sqrt{2}$. The transition between $|D\rangle$ and $|B\rangle$ can be occurred by applying the resonant RF fields, which results in splitting into quantum states dressed by the RF fields as shown in Fig.1(a). As the temperature increases, the resonant frequency of RF-dressed state shifts due to the change in the zero-field splitting - 74.2 K/$\sqrt{Hz}$. Therefore, a temperature change can be estimated by measuring the temperature shift of RF-dressed state observed in CW-ODMR spectra. The CW-ODMR spectra were measured by simultaneous application of continuous-wave of laser, MW, and RF fields as shown in Fig.1 (b).

Results and Discussion

Fig.1(c) shows the observed CW-ODMR spectra with the RF fields under the application of the transverse magnetic fields. It is found the 4 peaks are clearly observed, which confirms the creation of RF-dressed states. The estimated sensitivity of the temperature sensing is calculated to be 73.0 mK/$\sqrt{Hz}$ under the optimal conditions for the laser power, MW and RF field intensities, and this value is 6 times better than that with the conventional scheme. This is because the linewidth becomes narrower by suppressing the effect of the strain variations with increasing RF intensity. Moreover, the sharp dip structure observed in the CW-ODMR contributes to improving the sensitivity.
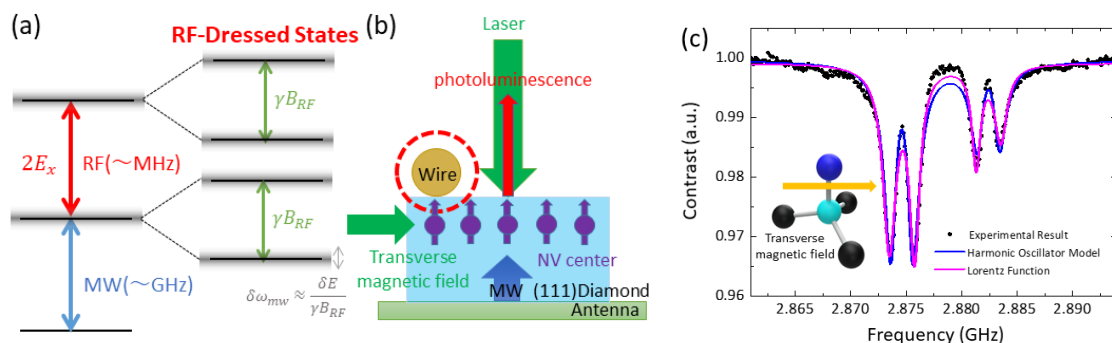

FIG. 1. (a) The energy diagram of our system (b) Experimental setup to measure the CW-ODMR (c) Experimental Result

Reference

[1]T. Yamaguchi, *et al*., Jpn. J. Appl. Phys., **58**, 100901 (2019).[2]Y. Matsuzaki, *et al*., J. Phys. Condens. Matt., **28**, 275302 (2016).
[3]K. Hayashi, *et al*., Phys. Rev. Appl., **10**, 034009 (2018). [4]S. Saijo, *et al*., Appl. Phys. Lett., **113**, 082405 (2018).

High-quality lead-vacancy centers in diamond by high-pressure and high-temperature annealing

Peng Wang[1], Takashi Taniguchi[2], Yoshiyuki Miyamoto[3], Mutsuko Hatano[1] and Takayuki Iwasaki[1]

[1]*Department of Electrical and Electronics Engineering, School of Engineering, Tokyo Institute of Technology*

[2] *International Center for Materials Nanoarchitectonics, NIMS, Japan*

[3] *Research Center for Computational Design of Advanced Functional Materials, AIST, Japan*

wang.p.ac@m.titech.ac.jp

Introduction

Color centers in diamond have aroused great interests nowadays: especially heavy group-IV vacancy centers in diamond are expected to possess sharp Zero phonon lines (ZPLs) and predicted long spin coherence times[1], serving as promising candidates for quantum network. However, the heavy atom (such as lead atom) suffers from difficulty in introducing into the diamond lattice during ion implantation, resulting in strong strained environment around lead vacancy (PbV) center. Such strained environment resulted in broad florescent emission, making it difficult to investigate properties of the PbV center. In order to observe its energetic structure and move forward to wavelength tuning or spin measurement, there is an urgent demand for high quality PbV whose fine structure could be clearly demonstrated, which requires an efficient approach to release the strain and recover defects formed during ion implantation.

Method and Results

For the fabrication of high-quality PbV centers in diamond, we adopted high-pressure and high-temperature (HPHT) annealing after Pb ion implantation, at 2100℃ under 7.7 GPa. Such a high temperature is considered to reduce the strain and recover defects in diamond, while the high-pressure condition maintains the stable phase of diamond. The same procedure has been proved to reduce inhomogeneous distribution of tin-vacancy center in diamond[1,2].

We show a sharp and clear spectrum of single PbV at around 6 K, in which the linewidth of C-transition was limited to the spectrometer[3]. By recording Hanbury Brown-Twiss (HBT) measurement at varying excitation powers, the single configuration was confirmed by antibunching, and we were able to estimate the excited state lifetime according to time correlation[4], ~3.7 ns, as shown in Fig. 1. Besides, our major concern is the strained environment around PbVs, which can be evaluated by their spectral distribution. We depicted the inhomogeneous distribution of the C-transition, which turned out a linewidth of 155 GHz, as shown in Fig. 2. Compared with former reported distribution of 10 nm with 950℃ annealing[5], our experimental results indicated that the inhomogeneous energetic distribution of PbVs were suppressed by HPHT annealing. Such narrow distribution is of vital importance for further research on photon indistinguishability.
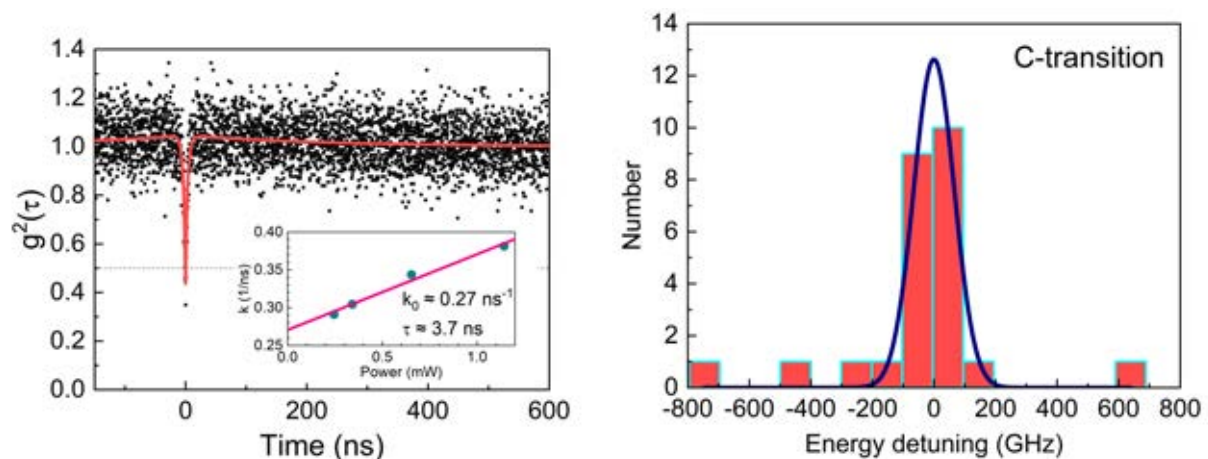
Fig.1 Estimated excited state lifetime of a single PbV

Reference

1. Iwasaki, T. *et al.* Tin-Vacancy Quantum Emitters in Diamond. *Phys. Rev. Lett.* **119**, 253601 (2017).
2. Goerltz, J. *et al.* Spectroscopic investigations of negatively charged tin-vacancy centres in diamond. *New J. Phys.* **22**, 013048 (2020).
3. Wang, P., Taniguchi, T., Miyamoto, Y., Hatano, M. & Iwasaki, T. Low-Temperature Spectroscopic Investigation of Lead-Vacancy Centers in Diamond Fabricated by High-Pressure and High-Temperature Treatment. *ACS Photonics* **8**, 2947–2954 (2021).
4. Khalid, A. *et al.* Lifetime Reduction and Enhanced Emission of Single Photon Color Centers in Nanodiamond via Surrounding Refractive Index Modification. *Sci. Rep.* **5**, 11179 (2015).
5. Fröch, J. E. *et al.* Versatile direct-writing of dopants in a solid state host through recoil implantation. *Nat. Commun.* **11**, 5039 (2020).

4th IFQMS

QUANTUM
INNOVATION
2021

Magnetocardiography imaging of living rats using NV centers in Diamond

Ryoma Matsuki[1], Keigo Arai[1,2], Akihiro Kuwahata[3], Daisuke Nishitani[1], Ikuya Fujisaki[1], Yuki Nishio[1], Zonghao Xin[3], Xinyu Cao[3], Yuji Hatano[1], Shinobu Onoda[4], Chikara Shinei[6], Masashi Miyakawa[6], Takashi Taniguchi[6], Masatoshi Yamazaki[7,8], Tokuyuki Teraji[5], Takeshi Ohshima[4], Mutsuko Hatano[1,4], Masaki Sekino[3], and Takayuki Iwasaki [1]

[1]*Department of Electrical and Electronics Engineering, School of Engineering, Tokyo Institute of Technology*
[2]*Japan Science and Technology PRESTO, Saitama, 332-0012, Japan*
[3]*Graduate School of Engineering, The University of Tokyo, Tokyo, 113-8656, Japan*
[4]*National Institutes for Quantum and Radiological Science and Technology, Takasaki, 370-1292,Japan*
[5]*Research Center for Functional Materials, National Institute for Materials Science, Tsukuba, 305-0044, Japan*
[6]*International Center for Materials Nanoarchitectonics, National Institute for Materials Science, Tsukuba, 305-0044, Japan*
[7]*Department of Cardiology, Nagano Hospital, Soja, 719-1126, Japan*
[8]*Medical Device Development and Regulation Research Center, The University of Tokyo, Tokyo, 113-8656, Japan*
matsuki.r.aa@m.titech.ac.jp

Introduction

Diamond quantum sensors based on nitrogen-vacancy (NV) centers have high spatial resolution operated at room temperature even under large background magnetic fields. We constructed a sensor system suitable for bio-magnetic measurement that can take advantage of the ability to bring the NV center closer to the signal source under ambient operating conditions. In this study, we introduce magnetocardiography(MCG) signal, mm-scale MCG imaging, and reconstruction of current in living rats.[1].

Experimental procedures and Results

We constructed a compact sample holder that allows the distance between a live rat heart and a diamond sample to be as close as about 1 mm as shown Fig.1(a), and measured MCG of living rats. Moreover, we conducted MCG imaging at 11x11=121 measurement points over 30 mm by automatically moving the XY stage with rats on it, and reconstructed the current density using bfieldtools[2,3] an open-source Python software suite. As a result, we measured MCG in a living rat at several tens of nT as shown Fig. 1(b), and reconstructed the current density distribution from MCG imaging with mm-scale spatial resolution as shown Fig. 1(c)(d). In addition, we conducted experiments with multiple rats using this sensor system, and confirmed that similar results could be obtained.

Acknowledgments

Reference

[1] K.Arai et al., arxiv:2105.11676(2021).
[2] Mäkinen, A. J. et al., J. Appl. Phys.128, 063906 (2020)
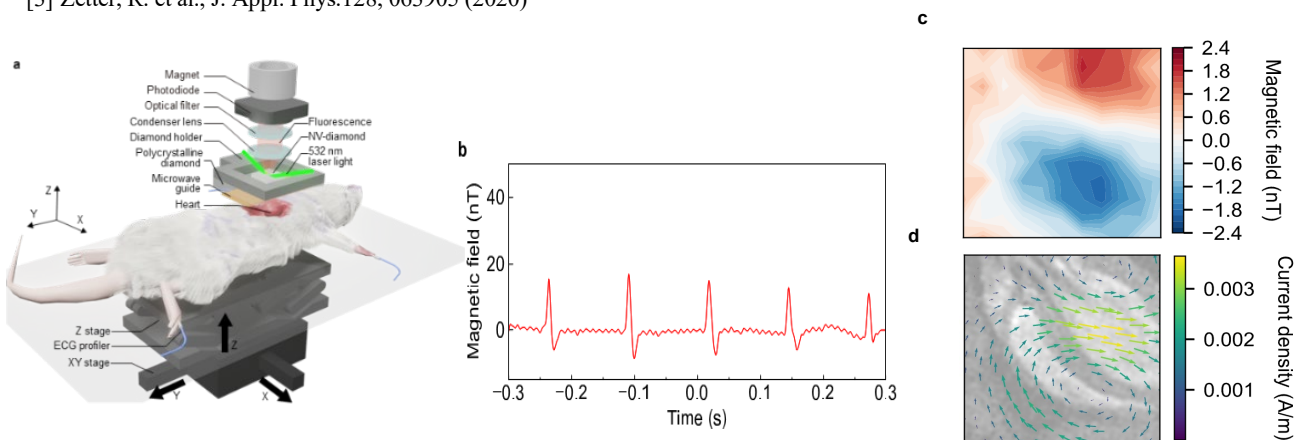[3] Zetter, R. et al., J. Appl. Phys.128, 063905 (2020)

Fig.1   (a) Schematic of the rat MCG setup.   (b) MCG signal from a rat.
   (c) (d) MCG imaging and reconstructed current distribution combined with MRI.

Probing correlated phenomena in 2D materials with diamond quantum sensors

Mark J.H. Ku[1]

[1]*Department of Physics and Astronomy and Department of Materials Science and Engineering, University of*

Delaware

mku@udel.edu

Understanding correlated spin and charge phenomena presents a rich arena for discovering exotic behaviors in materials and plays a critical role in developing next-generation information processing capabilities. 2D systems realized with van der Waals materials provide particularly interesting platforms for exploring correlated phenomena because of novel effects associated with reduced dimensionality and the opportunity for drastic miniaturization and for creating new functionality. Hence, understanding correlated phenomena in 2D materials is a frontier in condensed matter physics; however, this effort encounters numerous challenges related to measurement techniques, including spatially-varying current or spin distribution, small device dimension, and complex device geometry (e.g. heterostructure. Due to the ability to image magnetic field from current and spins with high spatial resolution over wide temperature range, quantum sensing with nitrogen-vacancy (NV centers in diamond provides a transformative tool for studying condensed matter phenomena. In this talk, I will discuss two topics in 2D materials probed with NV quantum sensing. We have directly imaged viscous flow of the Dirac electron fluid in graphene via NV magnetic imaging [1]. Understanding of the Dirac fluid presented in this work provides insight into strongly-correlated electrons such as those in high-temperature superconductors. Via NV magnetic imaging, we have also directly established room-temperature ferromagnetism in exfoliated flakes of Fe_5GeTe_2 (FGT [2] for the first time as well as in Co-doped FGT (Co-FGT. As a step towards detecting magnons (spin excitations in 2D magnets, we have also obtained the first ferromagnetic resonance measurement of Co-FGT bulk crystal. These results contribute towards the applications of 2D magnets in technologies and devices.

References

[1] M.J.H. Ku, T.X. Zhou, Q. Li, Y.J. Shin, J.K. Shi, C. Burch, L.E. Anderson, A.T. Pierce, Y. Xie, A. Hamo, U. Vool, H. Zhang, F. Casola, T. Taniguchi, K. Watanabe, M.M. Fogler, P. Kim, A. Yacoby, and R.L. Walsworth, *Nature* <u>583</u>, 537 (2020).

[2] Hang Chen, Shahidul Asif, Matthew Whalen, Jeyson Tamara-Isaza, Brennan Luetke, Yang Wang, Xinhao Wang, Millicent Ayako, Andrew F. May, Michael A. McGuire, Chitraleema Chakraborty, John Q. Xiao, and Mark J.H. Ku, *arXiv*:2110.05314 (2021).

Electroluminescence Observation of NV Center in Diamond Lateral p-i-n Diode

Moriyoshi Haruyama[1], Hiromitsu Kato[1], Masahiko Ogura[1], Yukako Kato[1], Takayuki Iwasaki[2], Norikazu Mizuochi[3], and Toshiharu Makino[1]

[1] *National Institute of Advanced Industrial Science and Technology*

[2] *Department of Electrical and Electronics Engineering, School of Engineering, Tokyo Institute of Technology*

[3] *Institute for Chemical Research, Kyoto University*

haruyama.moriyoshi@aist.go.jp

Introduction

Nitrogen Vacancy (NV) center in diamond is one of the most studied color centers. Especially in negatively charged NV center (NV^- center), electron spin state initialization and readout can be easily performed by laser irradiation. On the other hand, electrical manipulation of NV center without laser is required for chip-scale quantum device development. In 2013, two papers were reported about electroluminescence of NV center, however electrical excitation of NV^- center was not realized. It can be expected that charge state of NV^- center was stabilized by increasing electron concentration around NV center. To realize this, we fabricate high concentration phosphorus doped n layer. In this study, we tried observation of electroluminescence from NV center in the lateral p-i-n diode and investigate the electroluminescence characteristics.

Method

We fabricated p-i-n diode by using microwave plasma enhanced chemical vaper deposition (CVD) method. The i layer was grown on the (111) Ib high pressure high temperature diamond substrate. The i layer was slightly doped phosphorus to stabilize charge state of NV^- center (P concentration: 10^{16} cm^{-3}). Patterned boron doped p+ and phosphorus doped n+ layer were grown on the i layer. Both of boron and phosphorus concentration in p+ and n+ layer was 10^{20} cm^{-3}. After CVD growth, we performed nitrogen ion implantation and post-annealing to create NV center. Acceleration energy, ion fluence and implantation temperature were 350 keV 5×10^8 cm^{-3} and 600ºC, respectively. Post-annealing temperature and time were 850ºC, 30 min, respectively. After post-annealing, boiled acid mixture treatment (H_2SO_4 and HNO_3) was performed to terminate surface with oxygen. Electrode (Ti / Pt / Au) was created on both p+ layer and n+ layer.

Results

Figure 1 (a) and (b) shows PL and EL CFM map in i layer. The EL measurement was performed under applied 30V of forward bias. As shown in these figure, isolated luminescent centers were observed at same position. Figure 1 (c) and (d) show PL and EL spectra of luminescence center. Zero phonon line of NV^- center was detected from PL spectrum, while zero phonon line of NV^0 center was detected from EL spectrum. In these results, we succeed in electroluminescence observation of NV center by using lateral p-i-n diode. In presentation, we will report analysis result about NV^- component in the EL spectrum.
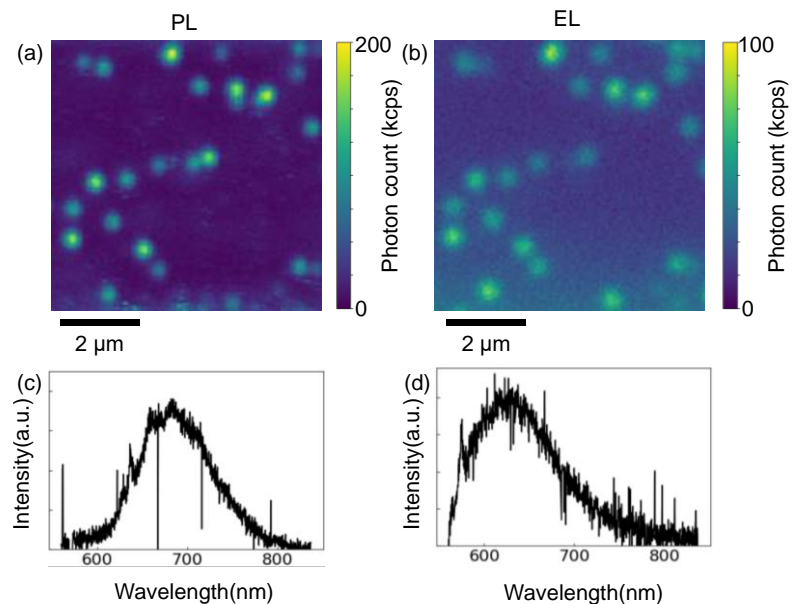

FIG. 1. (a) PL CFM map. (b) EL CFM map. (c) PL spectrum. (d) EL spectrum.

Reference

[1]N. Mizuochi et al., *Nature Photonics*, 6, 299 (2012)

[2]A. Lohrmann et al., *Applied Physics Letter*, 99, 251106 (2011)

4th IFQMS · QUANTUM INNOVATION 2021

Synthesis of HPHT diamond with controlled nitrogen concentration

Masashi Miyakawa[1], Chikara Shinei[1], Takashi Taniguchi[2], and Tokuyuki Teraji[1]

[1] *Research Center for Functional Materials, National Institute for Materials Science*

[2] *International Center for Materials Nanoarchitectonics, National Institute for Materials Science*

MIYAKAWA.Masashi@nims.go.jp

Introduction

For developing quantum sensing devices, it is essential to utilize diamonds containing NV center with desired concentration. The desired concentration of NV centers varies from 1 ppb to 10 ppm, depending on applications in quantum sensing devices. Thus, control of NV center concentration with a wide range is requested in diamond growth method. In case of diamonds grown under high-pressure and high-temperature (HPHT), NV centers are usually formed by electron beam irradiation to nitrogen-doped diamonds followed by post-annealing treatments. Here, precise control of the substitutional nitrogen (P1) center concentration during HPHT growth process with a wide range is a key for the concentration control of NV center. There were reports that nitrogen impurity was reduced to the limit by adding a nitrogen getter of Ti or Al,[1-4] but continuous control of nitrogen concentrations in wide range of the order of 100 to 0.1 ppm was not. In this paper, we will report the controllability of the nitrogen in the HPHT diamond synthesized with Co-Ti and Fe-Co-Ti base solvents by using Ti as a nitrogen getter.

Method

Single-crystalline diamonds were grown in Co-Ti and Fe-Co-Ti solvents by a temperature-gradient method using a modified belt-type high-pressure apparatus. Graphite and diamond with different boron impurity levels were used as carbon sources. Pressure, temperature, and growth duration were 5.5 GPa and 1350ºC for 40~80 h. Concentration of the P1 center was evaluated by electron spin resonance (ESR) measurements using a piece of diamond with (111) faces obtained by cutting parallel to (111) plane.

Results and discussion

ESR measurements indicated P1 center concentrations were exponentially decreased from 100 ppm to 0.1 ppm with increasing amount of Ti additives in the Co-Ti solvent, which provides the nitrogen concentration in diamond crystals can be controlled by optimizing amount of Ti additive. In the Fe-Co-Ti solvents, P1 concentration was decreased from ~90 ppm to ~0.08 ppm with increasing amount of Ti additive up to 2 wt%, and efficiency of nitrogen gettering by Ti additives was higher compared with the Co-Ti solvents. Moreover, it was found that selection of carbon source became important when the P1 concentration < ~0.2 ppm. The result of SIMS measurements indicated that residual boron concentrations in the grown diamonds were ~0.2 ppm when graphite was used as a carbon source and ~0.02 ppm when CVD diamond was used. Residual boron compensates for the P1 center, leading to an unexpected lower concentration of the P1 centers in the grown diamonds. Therefore, utilizing a high-purity carbon source such as CVD diamonds was found to be efficient for suppressing contamination by boron impurities in the synthesized diamonds with the P1 concentration < ~0.2 ppm.

Reference

[1]H. Sumiya, S. Satoh, Diam. Relat. Mater., 5, 1359 (1996).
[2]R.C. Burns, J.O. Hansen, R.A. Spits, M. Sibanda, C.M. Welbourn, D.L. Welch, *Diam. Relat. Mater.*, 8, 1433 (1999).
[3]H. Kanda, *Braz. J. Phys.*, 30, 482 (2000).
[4]A. D'Haenens-Johansson, K.S. Katrusha, P.J. Moe, W. Wang, *Gems Gemol.*, 51, 260 (2015).

Acknowledgements

4th IFQMS   QUANTUM INNOVATION 2021

SE-03A-β1-04

Formation of diamond film containing perfectly aligned NV center ensembles at a high growth rate by high-power density plasma CVD

Takeyuki Tsuji[1], Hitoshi Ishiwata[1,2], Takeharu Sekiguchi[1], Takayuki Iwasaki[1], and Mutsuko Hatano[1]

[1]Department of Electrical and Electronics Engineering, School of Engineering, Tokyo Institute of Technology

[2]PRESTO, Japan Science and Technology Agency

tsuji.t.ac@m.titech.ac.jp

Diamond film sensors with large volumes (> $(0.5 \text{ mm})^3$) containing perfectly aligned nitrogen-vacancy (NV) ensembles performing high contrast ($\approx$ 30%) are a promising material for achieving highly sensitive quantum magnetometers such as magnetoencephalography. The step-flow growth mode in which diamonds grow laterally by microwave plasma chemical vapor deposition (MPCVD) is required to realize aligned NV center ensembles. However, the conventional growth rate of aligned NV center ensembles was limited to a low value (0.05~ 0.5 μm/h) because a low gas flow ratio CH_4 / H_2 (< 0.5%) is needed for step flow growth [1–3]. In addition, the nitrogen density of the NV center film should be controlled to below 30 ppm to obtain high contrast because the high nitrogen densities shorten the life-time of the excited-state and reduce spin polarization, which leads to decreased the contrast [4].

In this study, we achieved a high growth rate (6.6 μm/h) of diamond film containing perfectly aligned NV ensembles with high contrast (30%) by applying high power density plasma (103 W/cm^3) and precisely controlling the flow rate ratios of CH_4 / H_2 and N_2 / CH_4. For introducing high power density plasma, we used an MPCVD with a spherical chamber to reflectively concentrate microwaves on the diamond stage with a microwave antenna, and higher gas pressure up to 30 kPa was introduced to concentrate the plasma on the diamond substrate. The power density was varied as 42, 66, 103 W / cm^3, which belongs to the high-density regime (> 40 W/cm^3) among the previous diamond CVD studies [5]. The growth temperature of 800 °C and growth time of 4 hours are fixed during the CVD growth.

The three-dimensional island growth was observed at the CH_4 / H_2 of 0.32% because of the nucleation formed on the terraces. Then, the hydrogen etching of the nucleation formed on the terraces was induced by decreasing the CH_4 / H_2 to below 0.16% leading to step-flow growth. Fig.1 shows that the growth rate of the diamond films with step flow growth were increased as the power density was increased. It was considered that increasing the power density, which can produce a large amount of carbon precursors while maintaining a low CH_4 / H_2 of 0.16%, realized step-flow growth, leading to a high growth rate (6.6 μm/h) with perfectly aligned NV center ensembles. The N_2 / CH_4 ratio was also controlled to be lower than 2.5%, and the nitrogen density in the diamond film was kept below 30 ppm to obtain a high Rabi contrast (30%) as shown in Fig2. Moreover, we measured the T_2^* of the obtained diamond sensor films by the high growth rate with the Ramsey sequence using a large detection volume of approximately 8000μm^3. We confirmed that T_2^* (= 210 ns) obtained in this study is mainly limited by nitrogen electron spin bath density of the diamond film (24 ppm) [6] and no significant decrease in T_2^* due to the deterioration of the crystallinity of the diamond film including strain gradients was observed. This result is promising for building material technology for highly sensitive quantum sensors with large sensor volumes.
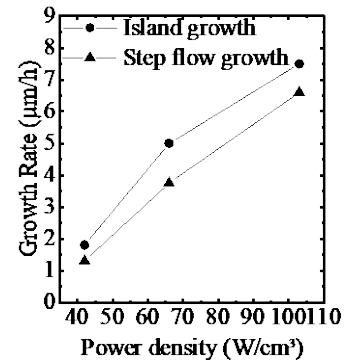

Fig.1. (a) Evolution of the growth rate of the CVD diamond films with island growth (triangular red dots) or the step-flow growth (circle black dots) as a function of the MW power density.
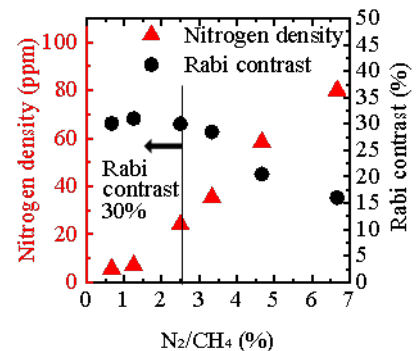

Fig.2. The nitrogen density in the CVD film (circle blue dots) and Rabi contrast (triangular red dots) dependence on N_2 / CH_4. To obtain high contrast ($\approx$ 30%), N_2 / CH_4 was controlled to be lower than 2.5%.

Acknowledgment

Reference

[1] H. Ozawa, K. Tahara, H. Ishiwata, M. Hatano, and T. Iwasaki, Appl. Phys. Express **10**, 045501 (2017).

[2] H. Ishiwata, M. Nakajima, K. Tahara, H. Ozawa, T. Iwasaki, and M. Hatano, Appl. Phys. Lett. **111**, 043103 (2017).

[3] P. Balasubramanian, C. Osterkamp, Y. Chen, X. Chen, T. Teraji, E. Wu, B. Naydenov, and F. Jelezko, Nano Lett. **19**, 6681 (2019).

[4] K. Mizuno, M. Nakajima, H. Ishiwata, M. Hatano, and T. Iwasaki, Appl. Phys. Express **14**, 032001 (2021).

[5] T. Teraji, T. Yamamoto, K. Watanabe, Y. Koide, J. Isoya, S. Onoda, T. Ohshima, L. J. Rogers, F. Jelezko, P. Neumann, J. Wrachtrup, and S. Koizumi, Phys. Status Solidi **212**, 2365 (2015).

[6] E. Bauch, S. Singh, J. Lee, C. A. Hart, J. M. Schloss, M. J. Turner, J. F. Barry, L. M. Pham, N. Bar-Gill, S. F. Yelin, and R. L. Walsworth, Phys. Rev. B Condens. Matter **102**, 134210 (2020).

High dynamic range current detection using a diamond quantum sensor

Yuta Shigenobu[1], Yuji Hatano[1], Jaewon Shin[2], Junya Tanigawa[2], Akimichi Nakazono[2],

Shinobu Onoda[3], Takeshi Oshima[3], Keigo Arai[1], Mutsuko Hatano[1, 3], Takayuki Iwasaki[1]

[1]Department of Electrical and Electronics Engineering, School of Engineering, Tokyo Institute of Technology

[2]Yazaki Corporation,

[3]National Institutes for Quantum Science and Technology

Shigenobu.y.aa@m.titech.ac.jp

Introduction

High dynamic range current detection is required to estimate the remaining charge in the battery and precisely predict the travelable mileage of EV. The maximum current flowing bus-bars connecting the battery will reach to several hundred amperes. Simultaneously, the measurement with 10 mA accuracy in the well-controlled temperature is required to expand the travelable mileage up to 10 %[1]. Thus, 5-digit dynamic range current sensor is crucial to realize an efficient battery system. In this study, to meet these requirements, we constructed a quantum sensor system using ensemble NV centers in diamond.

Method

Experimental set-up to measure the bus-bar current with the diamond sensor is shown in FIG.1. The diamond sensor used was a (111) type-Ib HPHT crystal, with a size of $2.0 \times 2.0 \times 1.0$ mm^3 and 3.0×10^{18} cm^{-2} EB irradiation. The sensor was attached to one end of a multi-mode fiber to excite by green laser and to collect the red fluorescence from the NV centers. The diamond sensor was placed perpendicular to the bus-bar to coincide the current magnetic field direction with the N-V axis. Since the magnetic field strength in the diamond sensor generated by the 1000 A bus-bar current was estimated to be 9 mT, 15 mT static magnetic field was applied by Nd magnets. The magnetic field was measured as the difference in the lock-in-amplifier (LIA) outputs in the two resonance frequencies generated by the microwave signal generator (SG)[2].

Result

The obtained spectrum of the magnetic field noise measured when SG and LIA were modulated by the frequency of F_{mod} = 20 kHz and the depth of F_{dev} = 3.5 MHz is shown in FIG.2. The noise floor of the sensor system was less than 10 nT/$\sqrt{Hz}$. This value is enough to measure the magnetic field generated by the 10 mA around the bus-bar. The current measurement procedure was as follows. The feedback path from LIA through integrator circuit to SG in FIG.1 is always stable if the magnetic field variation caused by the bus-bar current is within a few MHz, which we define as D, where the slope of CW-ODMR around the resonance frequency is monotonous. For the small range, a current pulse train with changing amplitude from 100 mA to 10 mA was applied and the 10 mA pulse could be detected as the change of the integrator output. Even if the current change was over D, the feedback was kept stable by repeating the intermittent adjustment of the center frequency of SG when the integrator circuit output reaches a predetermined value below D (for example, $D/2$). The current was incremented or decremented with 30 A amplitude and 2 s width steps. We confirmed that the feedback path could track the current variation up to $\pm$1000A provided.

This work was supported by MEXT Q-LEAP Grant Number JPMXS0118067395.

Reference

[1] H. Sugiyama et al., OP2, IFQMS3 (2020)   [2] Y. Hatano et al., Appl. Phys. Lett. 118, 034001 (2021)
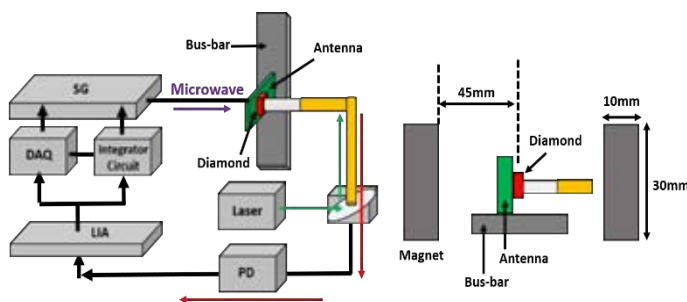
FIG.1 Experimental setup for measuring the bus-bar current with diamond sensor (left) and its expansion around the diamond sensor (right).
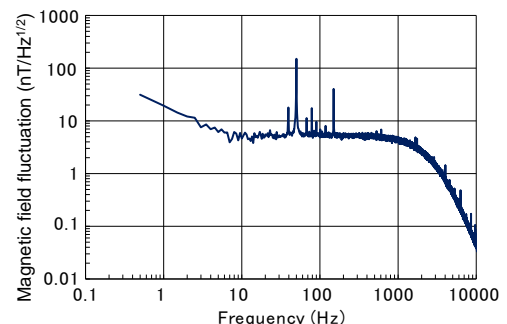

FIG.2 Measured noise spectrum of the diamond sensor at 15 mT magnetic field and 100 mW laser power.

4th IFQMS

QUANTUM INNOVATION 2021

Vector DC magnetic-field sensing with reference microwave field using a single nitrogen-vacancy center in diamond

Takuya Isogawa[1,*], Yuichiro Matsuzaki[2,†], and Junko Ishi-Hayase[1,‡]

[1]*Department of Applied Physics and Physico-Informatics, Keio University, Yokohama 223-8522, Japan*

[2]*National Institute of Advanced Industrial Science and Technology, Ibaraki 305-8568, Japan*

[*]tisogawa@keio.jp [†]matsuzaki.yuichiro@aist.go.jp [‡]hayase@appi.keio.ac.jp

Introduction

The measurement of DC magnetic fields at the nanoscale is important in various fields such as condensed matter physics [1]. In particular, a single nitrogen vacancy (NV) center in diamond is a promising device to achieve high sensitivity and spatial resolution. Recent studies have shown that vector DC magnetic-field sensing using a single NV center provides higher readout contrast and spatial resolution compared to conventional methods using NV center ensembles [2, 3]. However, these methods require the application of a reference DC field that may disturb the target system in order to estimate the azimuthal angle of the target magnetic field with respect to the NV axis. This can be a severe problem for materials that are sensitive to static magnetic fields. Here, we propose a scheme to measure vector DC fields without a reference DC field. The azimuthal angle of the target magnetic field can be measured from the Rabi frequency, using the direction of the microwave field to drive the Rabi oscillation as a reference. The proposed scheme delivers a novel technique for sensitive vector DC magnetic-field sensing with a single NV center.

Measurement of the azimuthal angle of the target DC magnetic field

The components perpendicular and parallel to the NV axis of the target magnetic field are estimated from the two resonance frequencies. While the azimuthal angle can be determined by applying a reference DC field to the system (Fig. 1a), our method provides a way to determine the azimuthal angle of the target field using the direction of the microwave as a reference (Fig. 1b). The perpendicular component of the target magnetic field tilts the quantization axis from the NV axis. When a linearly polarized resonant microwave is applied, Rabi oscillation occurs at the frequency proportional to the component of the microwave perpendicular to the quantization axis. Therefore, the tilt of the quantization axis can be determined from the Rabi frequency, and the direction of the applied DC magnetic field can be measured. Fig. 1c shows the sensitivity of the conventional scheme and our scheme. The simulation was performed by solving the master equation in the presence of Markovian dephasing. Here, we have used the same decay rate in the calculation of the sensitivity of both schemes. In the actual experiments, we expect that our scheme can achieve higher sensitivity because the coherence time of the Rabi oscillation is usually longer than that of the Ramsey interferometry.
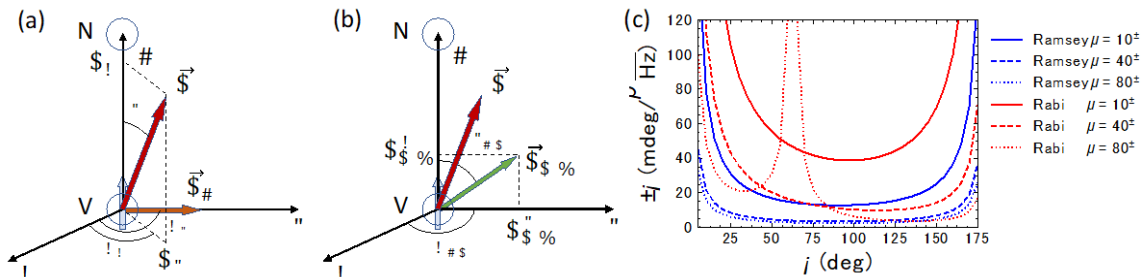

FIG. 1. (a) Configuration of NV axis, the target DC magnetic field, and the reference DC magnetic field. (b) Configuration of NV axis and the reference microwave field. (c) Sensitivity of the conventional scheme (blue) and our scheme (red) as a function of the azimuthal angle ϕ for $\theta = 10°$ (solid), $\theta = 40°$ (dashed), and $\theta = 80°$ (dotted). Here we fix $B = 8$ mT, $B_{\mathrm{mw}} = 1$ mT, $B_r = 1$ mT, and $\theta_{\mathrm{mw}} = 20°$. The decay rate is 1.0×10^6.

Acknowledgements

Reference

[1]F. Casola, T. Van Der Sar, and A. Yacoby, Nature Reviews Materials **3**, 1 (2018).
[2]X.-D. Chen, F.-W. Sun, C.-L. Zou, J.-M. Cui, L.-M. Zhou, and G.-C. Guo, Europhysics letters **101**, 67003 (2013).
[3]Y.-X. Liu, A. Ajoy, P. Cappellaro, Physical Review Letters **122**, 100501 (2019).

4th IFQMS

QUANTUM INNOVATION 2021

Thermal effects on generation of spin defects in hexagonal boron nitride

Tetta suzuki[1,2], Yuichi Yamazaki[2], Takashi Taniguchi[3], Kenji Watanabe[3],

Yu-Ichiro Matsushita[4], Yuta Masuyama[2], Yasuto Hijikata[1], Takeshi Ohshima[2]

[1]Saitama Univ, [2]QST, [3]NIMS, [4]Tokyo Tech

t.suzuki.838@ms.saitama-u.ac.jp

Introduction

There has been a lot of research on quantum sensors based on spin defects in wide gap semiconductors such as nitrogen-vacancy complex defect (known as NV center) in diamond, silicon vacancy in silicon carbide. Recently, hexagonal boron nitride (hBN), a 2D material, has been attracting attention as a new mother material for spin defect[1,2]. Energetic particle (electron, ion and neutron) irradiation is the most typical method to generate spin defects. However, such a method also introduce unnecessary defects degrading spin property of spin defect. Thermal treatment is a useful method to anneal residual defects. The effect after irradiation as well as during irradiation (high temperature irradiation) has been studied[3,4]. In this paper, we investigated the thermal effect on generation of boron vacancy defect (V_B) in hBN.

Method

We used hBN flakes on SiO_2/Si substrate formed by tape transfer method which is commonly used in graphene research. 40 keV-N_2 ions were irradiated with the optimized fluence of 1×10^{15} cm^{-2} at room temperature. Then, the irradiated sample was isochronally annealed up to 800 °C. For comparison, 40 keV-N_2 ion irradiation at elevated temperature up to 800 °C was carried out. The photoluminescence (PL) spectra were measured using a HORIBA LabRAM HR Evolition (laser wavelength: 532 nm, laser power: 0.1 mW). Optically detected magnetic resonance (ODMR) measurements were performed using a home-made confocal microscope. We used a software-based the lock-in detection for the ODMR measurements.

Result

PL intensity and ODMR signal contrast as a function of treatment temperature were shown in Fig. 1 and 2. In the post-annealing experiment, the PL intensity remained almost the same up to 400 °C and then began to decrease at 500 °C, finally disappeared above 600 °C. ODMR signal contrast showed the similar trend and was maximized on 400 °C annealed sample. On the other hand, for high temperature irradiation, the PL intensity was maintained up to 600 °C, and no PL was shown above 700 °C. The 600 °C irradiated sample showed higher ODMR signal contrast from all other samples. These results concluded that high temperature irradiation is also useful for spin defect in 2D material.
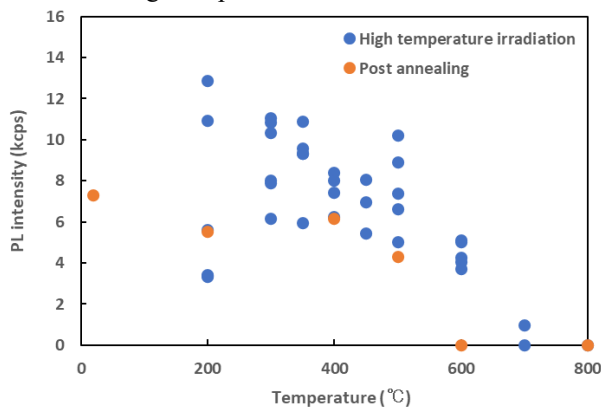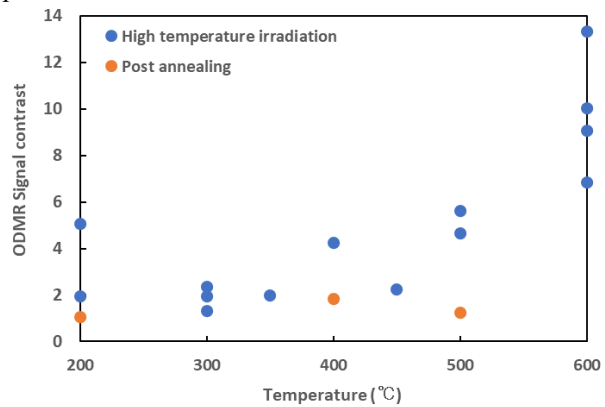

FIG. 1. Change of PL intensity

FIG. 2. Change of ODMR signal contrast

Acknowledgement

Reference

[1]A.Gottsholl et al., Nat Mater. 19, 540 (2020). [2]M.Kianinia et al., ACS Photonics. 7, 2147 (2020).
[3] M.Capelli et al., Carbon 143, 714 (2019). [4]Y.Chiba et al., Mater. Sci. Forum 1004, 337 (2020).

4th IFQMS

QUANTUM INNOVATION 2021

Error-Disturbance uncertainty relations in Faraday measurements

Le Bin Ho[1], and Keiichi Edamatsu[1]

[1]Research Institute of Electrical Communication, Tohoku University

binho@riec.tohoku.ac.jp

Introduction

Quantum measurement plays a crucial role in the characterization of physical systems, which elucidate hidden quantum properties to the classical world. One of its important intrinsic properties is the uncertainty relation which is infeasible to measure incompatible observables with arbitrary precision. Heisenberg was first formulated an uncertainty relation between the position and momentum and later generalized by Arthurs and Kelly

$$\epsilon_A \eta_B \geq \mathcal{C}_{AB},$$

that we call the Heisenberg-Arthurs-Kelly uncertainty. Here, ϵ_A is the error when measuring A and η_B is the disturbance causes to B measurement, $\mathcal{C}_{AB} = |\langle\psi|[A,B]|\psi\rangle|/2$, where $|\psi\rangle$ the system state to be measured.

Furthermore, Ozawa [1] and Branciard [2, 3], have considered a rigorous relation reads

$$\epsilon_A^2 \sigma_B^2 + \sigma_A^2 \eta_B^2 + 2\epsilon_A \eta_B \sqrt{\sigma_A^2 \sigma_B^2 - \mathcal{C}_{AB}^2} \geq \mathcal{C}_{AB}^2,$$

that hereafter we call the Branciard-Ozawa uncertainty, where $\sigma_\Lambda = \sqrt{\langle\Lambda^2\rangle - \langle\Lambda\rangle^2}$ represents the standard deviation of Λ.

Recently, Faraday measurements of spin based on an atom-light interface framework have been studied actively. It has contributed to our understating of quantum measurement of spin systems and has various applications in quantum metrology of atoms and spins, quantum information processing, strongly correlated systems, and many-body systems. The Faraday effect causes the rotation of the polarized light by the spin and thus allows indirect measurement of it via the polarized light. Such a measurement contains fundamental limits in the sensitivity caused by the quantum nature of light. Likewise, the back-action of the polarized light perturbs the spin state, which causes disturbance on the subsequent measurements of the spin. In this work, we formulate an atom-light interface scheme for evaluating uncertainty relations.

Method

The atom is a single spin-1/2 particle interacting with a classical coherent polarized light. In this way, we derive the error and disturbance, and observe the cyclic oscillations as a result of the Faraday rotation and spin rotation as show in Fig. 1. Due to the rotation of the polarized light, the square error first is gradually decreases and then gradually reduces to the minimum at $g = \pi/4$ and increases again at $g = \pi/2$. The behavior is then repeated when increasing g. Likewise, the square disturbance increases quadratically with the interaction strength and reaches the maximum at $g = \pi/2$ and then decreases to zero for g varies from 0 to π. This behavior is the imprint of the back-action effect on the spin system that disturbs (rotates) the spin on its Bloch sphere.

Similarly, we investigate the case of polarization squeezed light using the phase-space approximation for the light, where the squeezing parameter takes place as a measurement strength. Larger squeezed parameter means broader Gaussian shape in the class of the polarization squeezed state, which is equivalent to "weak measurement", while small squeezed parameter refers to the narrow of Gaussian shape which results in a strong measurement.

FIG. 1. The plot of the square error and square disturbance as functions of interaction strength.

We finally formulate the error-disturbance relations in these cases above and provide that the Heisenberg-Arthurs-Kelly uncertainty can be violated while the tight Branciard-Ozawa uncertainty [2] always holds.

In conclusion, we evaluated the error, disturbance and uncertainty relations in quantum measurement in the atom-light interface framework of Faraday measurements. Our analysis would contribute to the understanding of the error and disturbance as well as the uncertainty principle in the spin measurements under the atom-light interface framework.

Reference

[1] M. Ozawa, Error-disturbance relations in mixed states, arXiv:1404.3388 [quant-ph] (2014).

[2] C. Branciard, Proceedings of the National Academy of Sciences **110**, 6742 (2013).

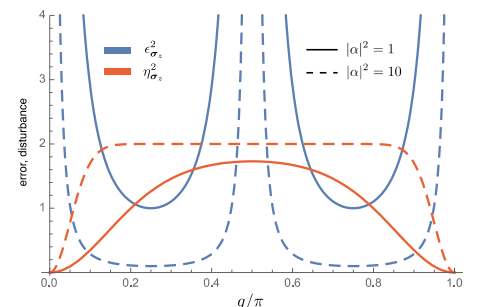[3] C. Branciard, Phys. Rev. A **89**, 022124 (2014).

4th IFQMS QUANTUM INNOVATION 2021

Hydrogen Annealing Effect on Silicon Optical Waveguide

Yixin Wang[1], Kohei Haji[2], Shunsuke Abe[2], Takuya Inagaki[2], Yoshiaki Kanamori[3],

Keiichi Edamatsu[1], Hirohito Yamada[2], Nobuyuki Matsuda[2]

[1]Research Institute of Electrical Communication, Tohoku University

[2]Department of Communications Engineering, Graduate School of Engineering, Tohoku University

[3]Department of Robotics, Graduate School of Engineering, Tohoku University

wangyixin@quantum.riec.tohoku.ac.jp

Introduction

In recent years, micro-optical waveguides such as silicon optical waveguides have been attracting attention for large-scale integration of optical circuits. The main cause of propagation loss in silicon optical waveguides is light scattering due to the roughness of the surface of the waveguide core, especially at the side walls [1]. It is expected that the propagation loss of the silicon optical waveguide will be improved by minimizing the roughness of the silicon surface. Hydrogen annealing has been reported as one of the effective techniques for smoothing the silicon surface [2]. In this work, we applied hydrogen annealing to a silicon optical waveguide and evaluated the effect on a silicon optical waveguide.

Method and Results

The channel waveguides were fabricated in 220-nm silicon on insulator (SOI) substrates. The resist pattern of the waveguides was formed by electron beam lithography. The pattern was transferred to silicon by using inductively-coupled plasma based reactive ion etching. The width of the waveguide was 440 nm, while both facets were designed to be as wide as 3 μm for the effective coupling between a lensed fiber and the waveguide for transverse-electric (TE) mode.

The waveguides chip was then annealed in a hydrogen atmosphere. The temperature, pressure and annealing time were 800 °C, 5 kPa and 2 minutes, respectively. The optical properties of the waveguides were measured with an amplified spontaneous emission (ASE) light source before and after annealing. FIG.1 shows the waveguide insertion loss as a function of the waveguide length. In the measurement the input ASE light was filtered by a 1 nm band-pass filter with the center wavelength of 1550 nm before the waveguide. We see that the propagation loss increased after annealing. By using the cut-back method, we estimate that the propagation loss increased by 14.5 dB/cm while the coupling loss of the waveguide decreased by 1.17 dB/facet. The possible cause of the increase in propagation loss is that silicon may be oxidized at a high temperature [3] due to the presence of oxygen contained in the exposed SiO_2 layer near the waveguide. FIG.2 shows the transmission spectra of the 1 cm long waveguide before and after annealing. After hydrogen annealing, the insertion loss of the waveguide increased significantly over the whole measurement range. However, the spectral ripple reduced after annealing, which may be due to the low Fabry-Perot interference caused by high propagation loss.
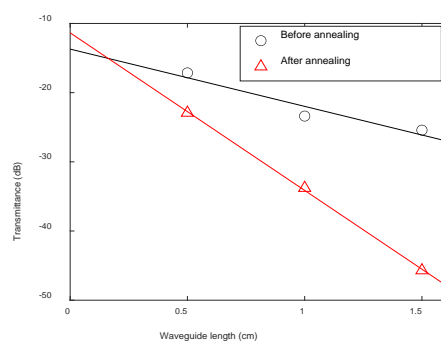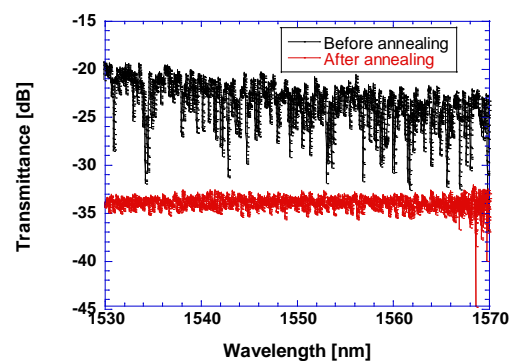

FIG. 1. Insertion loss vs. waveguide length.

FIG.2. Transmission spectra.

Acknowledgement

Reference

[1] T. Horikawa *et al.*, MRS Communications <u>6</u>, 9 (2016).

[2] T. Okatani *et al.*, Opt. Mater. Express <u>11</u>, 189 (2021).

[3] K. Hofman et al., Appl. Surf. Sci. <u>30</u>, 25 (1987).

Wavelength-tunable broadband infrared quantum absorption spectroscopy in the mid-infrared region 2-5 μm

Masaya Arahata[1], Yu Mukai[1], Toshiyuki Tashima[1], Ryo Okamoto[1], and Shigeki Takeuchi[1]

[1]*Department of Electronic Science and Engineering, Kyoto University, Japan*

arahata.masaya.34c@st.kyoto-u.ac.jp

Introduction

Infrared spectroscopy is a powerful technique enabling the noninvasive analysis of the dynamics of the molecular vibration and rotation modes, and an essential tool for material science and life sciences. However, a conventional infrared spectrometer has the problems that infrared light sources have large thermal noise and low directivity and infrared detectors need the cryogenic cooling for the high sensitivity. To overcome these problems, recently, infrared quantum absorption spectroscopy (IRQAS) has been proposed and experimentally demonstrated [1]. IRQAS enables the spectral measurement in the infrared region only with a low-cost and high-performance visible light source and detector using the quantum interference between the generation processes of entangled visible-infrared photon pairs. For the broadband IRQAS, some methods of broadening the generation bandwidths of photon pairs such as the group velocity phase matching were used to the IRQAS measurement [2]. However, the measurable wavelength ranges of IRQAS were limited to less than 1 μm at most. Therefore, there are no IRQAS systems covering the mid-infrared (MIR) region 2-5 μm.

Here, we report a wavelength-tunable IRQAS system covering the MIR region 1.9-5.2 μm. The generation wavelengths of visible-infrared photon pairs can be tuned by rotating a nonlinear crystal with respect to the pump beam to control the phase matching condition [3]. We show the quantum interference is observed in the wavelength region of 2-5 μm just by continuously rotating a crystal without the fine realignment. We also experimentally demonstrate the transmission spectrum measurement of a silica glass sample from the ratio of visibilities of interferogram with and without a sample. Furthermore, we demonstrate the transmittance measurement with a higher resolution with quantum Fourier-transform infrared spectroscopy (QFTIR), which enables the measurement in the whole spectrum of photon pairs from the Fourier analysis of the quantum interferogram [4].

Method

Figure 1 shows our experimental setup of wavelength-tunable IRQAS system with the continuous crystal rotation. A 0.5-mm-thick type-I MgO:LiNbO$_3$ crystal with a cut angle of 57.9° is pumped by a CW laser beam with a wavelength of 532 nm. The pump beam is focused into the crystal by a lens (f=200 mm). Signal (visible) photons with a wavelength of 692 nm and idler (infrared) photons with a wavelength of 2300 nm are generated in the case of the normal incidence of the pump beam on the crystal. The SPDC wavelengths can be tuned by rotating the crystal on a rotational stage with respect to the pump beam. When being separated by a dichroic mirror, the signal and pump photons pass through, while the idler photons are reflected. Then, the signal and pump photons are together reflected back to the crystal by a concave mirror (f=100 mm). The idler photons are collimated by a lens (f=100 mm) and then pass through an ultra-violet fused silica glass window with the thickness of 1 mm as a sample and are reflected by a mirror on a high-accurate translation stage with the position repeatability $\pm$2 nm. Then, at the crystal, the second SPDC generation process occurs by the reflected pump beam. After being collimated by a lens (f=250 mm) and passing through a long pass filter, an iris as a spatial filter, and a tunable band pass filter on a translation stage to eliminate the residual pump beam and the background light, signal photons are coupled to a multimode fiber and then guided to a Si avalanche photodiode and a photon counter to measure the interference of the single photon counts. In this presentation, we will report on the results of transmittance measurement of the sample with the wavelength-tunable IRQAS system. This work was supported in part by the foundation of MEXT Q-LEAP Grant Number JPMXS0118067634, JST-CREST Grant Number JPMJCR1674, JSPS KAKENHI Grant Number 21H04444, Grant-in-Aid for JSPS Fellows Grant Number 20J23408, and WISE Program, MEXT.
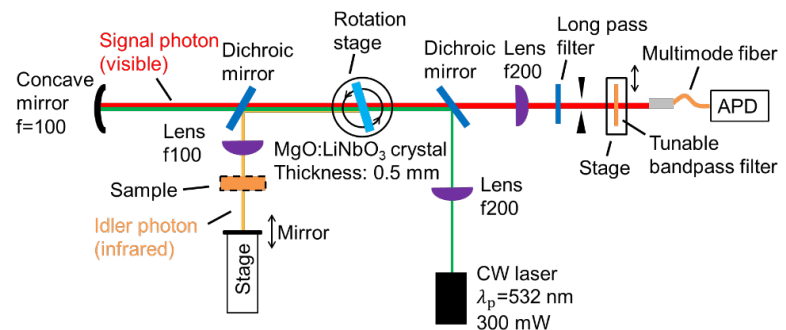

FIG. 1. Schematic of wavelength-tunable IR-QAS system. APD: Avalanche photodetector.

Reference

[1]D. Kalashnikov, A. Paterova, S. Kulik, and L. Krivitsky, *Nat. Photonics*, 10, 98 (2016).

[2]C. Lindner, J. Kunz, S. J. Herr, S. Wolf, J. Kießling, and F. Kühnemann, *Opt. Express*, 29, 4035-4047 (2021).

[3]M. Arahata, Y. Mukai, B. Cao, T. Tashima, R. Okamoto, and S. Takeuchi, *J. Opt. Soc. Am. B*, 38, 1934-1941 (2021).

[4]Y. Mukai, M. Arahata, T. Tashima, R. Okamoto, and S. Takeuchi, *Phys. Rev. Applied*, 15, 034019 (2021).

Evaluation of superconducting nanowire single photon detectors for mid-infrared wavelengths

Yuki Gama[1], Toshiyuki Tashima[1], Masaya Arahata[1], Yu Mukai[1], Fumihiro China[2], Masahiro Yabuno[2],

Satoru Mima[2], Shigeyuki Miyajima[2], Shigehito Miki[2], Hirotaka Terai[2], Ryo Okamoto[1], and Shigeki Takeuchi[1]

[1]*Department of Electronic Science and Engineering, Kyoto University*

[2]*National Institute of Information and Communication Technology*

takeuchi@kuee.kyoto-u.ac.jp

Introduction

Recently, single-photon detection in the mid-infrared spectral region has attracted attention as a fundamental technique for many technologies such as infrared quantum absorption spectroscopy[1,2] and light detection and ranging (LIDAR)[3]. However, the single-photon detectors operating in that region suffers from the limited operating wavelength and low detection efficiency. One of the solutions is to use superconducting nanowire single-photon detector (SNSPD) which possesses single-photon detection ability and low dark count. Some researchers have developed SNSPDs for the mid-infrared spectral region and, for example, Verma *et al.* evaluated the detection performance of SNSPDs fabricated from WSi up to a wavelength of 10 μm[4]. However, the detection efficiency of such mid-infrared single-photon detectors has not been fully evaluated so far. In this presentation, we report the experimental evaluation of a NbTiN SNSPD working in the mid-infrared spectral region. We evaluated dark count and the linearity of detection count by changing the input photon number and the bias current. We also investigated the detection efficiency and obtained the value of 1.20 ± 0.40 % at the wavelength of 4.33 μm with the bias current of 21.0 μA.

Method

We developed a NbTiN SNSPD for the mid-infrared single-photon detection. To improve the sensitivity for the mid-infrared single-photons, we fabricated the nanowire with thinner line width of 50 nm instead of typical 80 to 100 nm used for the SNSPD working in visible and telecommunication spectral region. The SNSPD also has a meander structure and the active area of 15×15 μm^2 (see figure 1(a) inset).

The experimental setup for evaluating SNSPD is shown in FIG. 1(a). We used quantum cascade laser (QCL) with a wavelength of 4.33 μm. The laser power was attenuated to the single photon level with the combination of neutral density filters and polarizers. The light was coupled to a single mode fiber and passed through a polarization controller which consists of a polarizer, a half-wave plate, and a quarter-wave plate. Using this system, the input photon polarization was optimized to maximize the detection count by the SNSPD. The output port of SNSPD was connected to an oscilloscope to observe the waveform of the output voltage pulse from SNSPD or a pulse counter to obtain the detection count. Here, FIG. 1(b) shows the waveform of the output voltage pulse from the SNSPD. We set threshold voltage of a pulse counter for each bias current with this result. Using these voltages, we evaluated dark count and the linearity of detection count by changing the input photon number and the bias current. In this presentation, we will report the evaluation results in more detail.
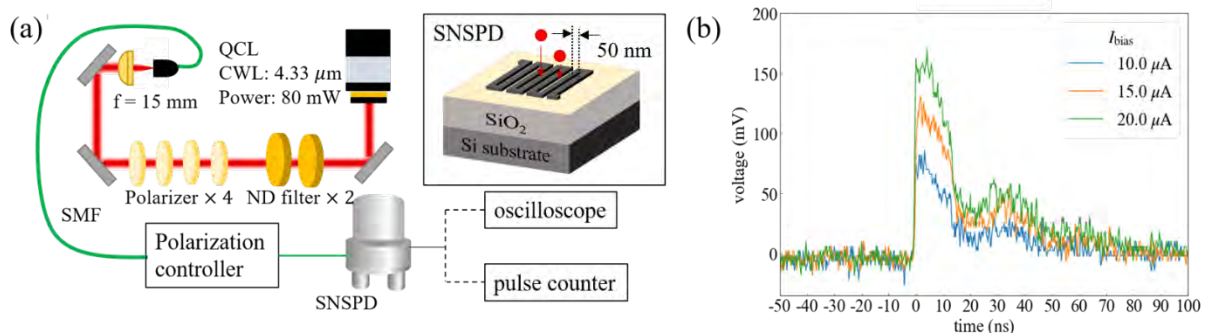
FIG. 1. (a) Experimental setup for the evaluation of mid-infrared SNSPD. ND filter: Neutral density filter, SMF: Single mode fiber. The inset shows the schematic of SNSPD. (b) The waveform of the output voltage pulse from mid-infrared SNSPD.

Reference

[1] D. Kalashnikov, A. Paterova, S. Kulik, and L. Krivitsky, *Nat. Photonics*, 10, 98 (2026).

[2] Y. Mukai, M. Arahata, T. Tashima, R. Okamoto, and S. Takeuchi, *Phys. Rev. Applied*, 15 (2021).

[3] G. Taylor, D. Morozov, N. Gemmell, K. Erotokritou, S. Miki, H. Terai, and R. Hadfield, *Opt. Express* 27 (2019)

[4] V. B. Verma *et al.*, *APL Photonics*, 6, 056101 (2021).

4th IFQMS

QUANTUM INNOVATION 2021

Phase retrieval of joint spectral amplitude

Kemeng Chen and Ryousuke Shimizu

The University of Electro-Communications Fundamental Science and Engineering

c2033074@edu.cc.uec.ac.jp

Introduction

  Tailored and energy tunable entangled photons are required rather than polarization entanglement on quantum information and communication technologies. To characterize the entanglement in a qubit system, such as polarization entanglement, quantum state tomography has been developed. On the other hand, the evaluation of entanglement for infinite dimension can be achieved by von Neumann entropy obtained by Schmidt decomposition. However, to implement Schmidt decomposition, the complex probability amplitude of a two-photon state should be required. Today, we can measure the two-photon spectral or temporal distributions in 2D space, but it is still challenging to evaluate phase distributions of the two-photon state. Here we develop Gerchburg-Saxton (GS) algorism to retrieve the phase distribution. In addition, the original intensity data should be corrected by Wiener filter to suppress the noise fluctuation of the retrieved data.

Method

  To implement GS algorism, we need a pair of data connected with Fourier transformation. Recently we proposed synthesizing time-frequency entangled photons and verified it by measuring joint spectral and temporal intensities. We applied GS algorism to these data in the following procedure.   At first, we added a random phase distribution to the frequency domain data and applied fast Fourier transform (FFT). Then, we extracted the transformed phase distribution in the time domain and reconstructed the joint temporal amplitude. Next, FFT was performed on the joint temporal amplitude repeatedly applied the same operation in the time and frequency domains. The transformed amplitudes were compared with the measured amplitudes and estimated an error. FFT was continued until the error values were below 5%, and eventually, the retrieved phase distribution was obtained. After the algorism was completed, the resolution of the measured data should be considered to correct the retrieved result. Compared with time-domain data, the resolution in the frequency domain can be ignored and the time domain resolution was about 200 fs. So, we created ten point-spread functions (PSF) and use the Wiener filter to recorrect the original data. While the noise signal rate is 18, the best retrieval result was shown as the resolution is 197 fs. Figure 2 shows the retrieved phase distribution extracting the area that exceeds 50% of maximum intensity. Additionally, the retrieved phase distribution can be used on Hong-Ou-Mandle (HOM) interference conjecture. We also tried to evaluate the visibility of the retrieved result and compare it to its HOM interference experiment result.
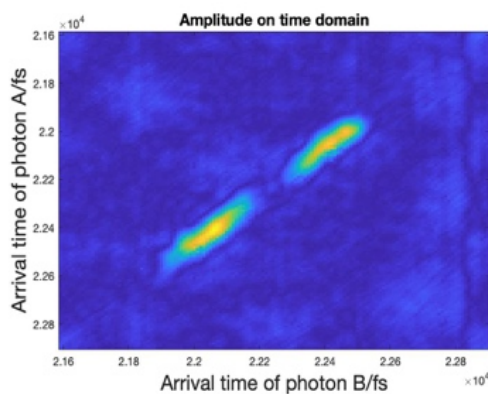
Fig. 1 Amplitude on time domain after phase retrieval and recorrected through point spectral function with 197 fs resolution
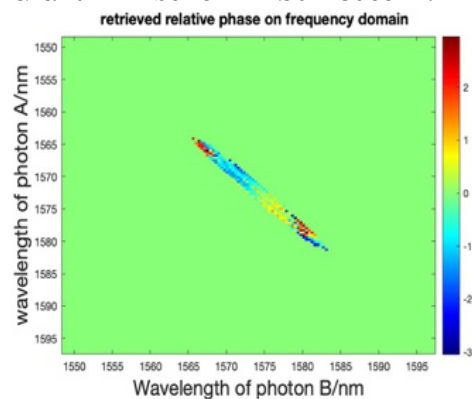

Fig. 2 Retrieved relative phase on frequency domain corrected by point spectral function with 197 fs resolution

Temporal shaping of an entangled-photon wave packet by Fourier optical synthesis

H. Oshima[1], F. China[2] M. Yabuno[2], S. Miki[2], H. Terai[2], and R. Shimizu[1]

[1]Univ. of Electro-Comm, [2]NICT

o2033021@edu.cc.uec.ac.jp

Introduction

   Temporal waveform control of ultrashort optical pulses is based on the one-dimensional Fourier transform relationship between the time and frequency domains, known as "optical synthesis" (OS). On the other hand, we have demonstrated that a two-dimensional Fourier transform (2D-FT) connects two-photon probability distributions of entangled photon pairs in time and frequency domains [1]. Based on this, we have developed manipulating the two-photon wave packet via 2D-FT, termed "quantum optical synthesis" (QOS) [2]. In this experiment, we created two discrete modes in 2D frequency space. However, the two-mode manipulation allows us to control the temporal waveform of entangled photons only in sinusoidal modulations. Our research aims to arbitrarily shape the time-domain structure of two photons with the 2D-FT manner. In this work, we present the extension of the frequency mode of the entangled photons toward arbitrary waveform shaping.

Method

   The experimental results are shown in Fig. 1. Figure 1 (a) is a two-photon spectral distribution, bidirectionally pumped for one nonlinear crystal. We can see two discrete frequency modes in the -45° direction. The corresponding temporal distribution of the two-photon is shown in Fig. 1(b), which has a sinusoidal modulation in the -45° direction. The temporal distribution with the sub-picosecond resolution was measured by up-conversion detection of single-photon with ultrashort pulses. Figure 1(c) is the measurement results obtained when creating four frequency modes using two nonlinear crystals. The corresponding time distribution is shown in Fig. 1(d). Setting the relative phase among all the frequency modes to be nearly 0, we can see slightly complicated temporal modulation as represented by $|\cos(2\pi \times 0.33\tau_-) + \cos(2\pi \times 1.0\tau_-)|^2$
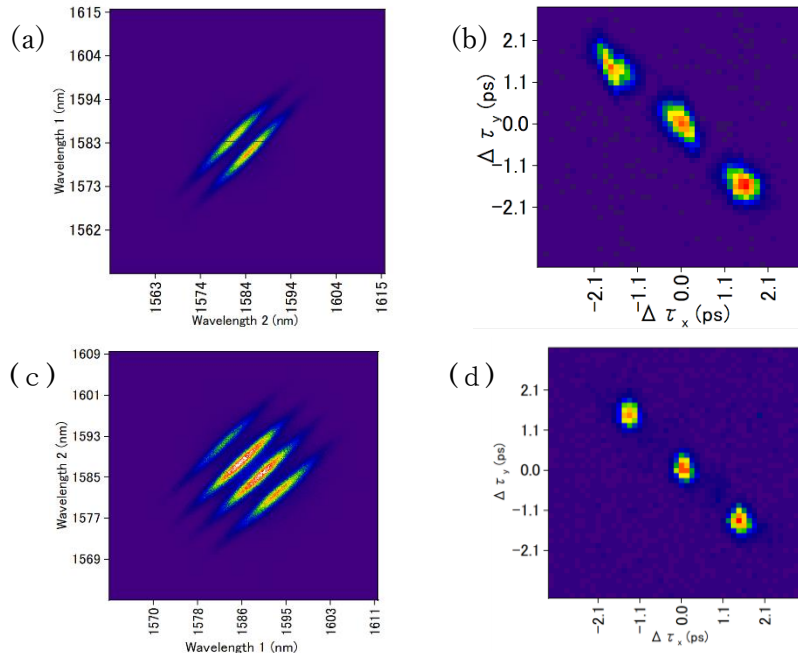
Fig.1 Upper plots are the experimental result of two-frequency mode (a) two-photon frequency and (b) temporal distribution. Lower plots are the experimental result of four-frequency mode (c) two-photon frequency and (d) its corresponding temporal distributions.

Reference
[1]R.-B. Jin, T. Saito, and R. Shimizu, Phys. Rev. Appl. **10**, 034011 (2018).
[2]R.-B. Jin, K. Mihoshima, R. Shimizu *et al*., APL Photonics **6**, 086104 (2021).

4th IFQMS

QUANTUM INNOVATION 2021

Cryogenic Monolithic Interferometer for Sensing Gravity Gradient

Satoru Takano[1], Ching Pin Ooi[1], Yuka Oshima[1], Yuta Michimura[1], and Masaki Ando[1]

[1]Department of Physics, School of Science, The University of Tokyo

satoru.takano@phys.s.u-tokyo.ac.jp

Introduction

Gravity gradient fluctuations are essential observation targets for precise measurement of motion of masses. From their measurement we obtain information about their source behavior. Recently fluctuations at low frequency, around 0.1 Hz, has been aimed for earthquake early alert using transient change of gravity potential [1] and for observation of GWs from mergers of intermediate-mass black holes [2].

A torsion-bar antenna (TOBA) is a ground-based gravity gradiometer proposed for measurement of gravity gradient fluctuations in such frequencies [2]. It measures torsional rotation angle of horizontally suspended mass(es) induced by gravity gradient fluctuations. Several prototypes and related technologies have been developed [3,4], and now we are planning to make a 30-cm scale prototype (Phase-III TOBA). Figure 1 shows the design setup of Phase-III TOBA

The goal of Phase-III TOBA is to achieve the strain sensitivity 10^{-15} / $\sqrt{\text{Hz}}$ at 0.1 Hz and demonstrate noise reduction, especially thermal noise by cooling the suspension system down to 4 K. To achieve this target sensitivity, reduction of sensing noise of interferometer is necessary. One solution is to make the readout system monolithically. Figure 2 shows the basic concept of the readout interferometer. We present development plan of the monolithic interferometer and current situation.

Method

Monolithic interferometer consists of optical components directly glued on a plate. Thanks to this configuration we can reduce readout noise caused by vibration of optical components, thermal drift, etc. On the contrary, unlike ordinary interferometers we cannot adjust optics after gluing. Therefore, its construction requires special care. Recently the technology of construction has been well studied and validity of noise suppression has been proved in many fields.

Monolithic interferometers have been studied for applications in room temperatures. However, for TOBA case the interferometer is under cryogenic environment. Therefore, we have to revise usual way of construction of monolithic interferometer in order to survive in cryogenic temperatures. We have tested alternatives suitable for cryogenic environment and the results will be reported in the presentation.
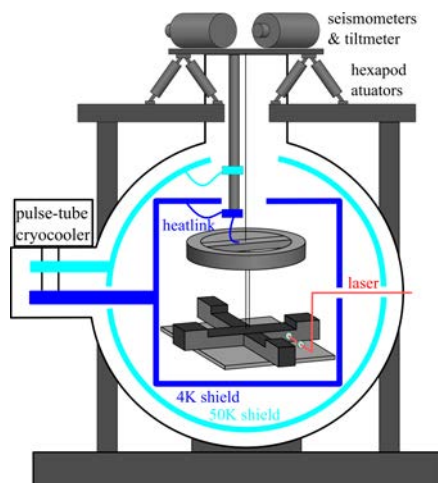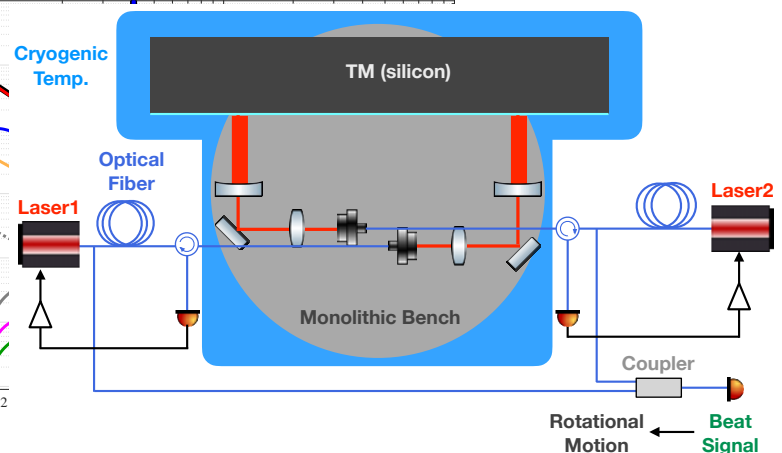

FIG. 1. Setup of Phase-III TOBA.

FIG. 2. Schematic of readout interferometer.

Reference

[1]J. Harms *et al*., *Geophys. J. Int.*, 201, 1416-1425 (2015) [2]M. Ando *et al*., *Phys. Rev. Lett.*, 105, 161101 (2010)
[3]K. Ishidoshiro *et al.*, *Phys. Rev. Lett.*, 106, 161101 (2011) [4]A. Shoda *et al.*, *Phys. Rev. D*, 95, 082004 (2017)

Suspension Noise measurements of Cryogenic Torsion Pendulums with Crystalline Fibres

Ching Pin Ooi[1], Satoru Takano[1], Yuka Oshima[1], Yuta Michimura[1], and Masaki Ando[1]

[1]*Department of physics, School of Science, The University of Tokyo*

ooichingpin@g.ecc.u-tokyo.ac.jp

Introduction

Thermal noise in mechanical sensors are a fundamental noise source and a limit for sensitivity. Torsion Bar Antenna (TOBA), a proposed ground-based gravity gradiometer targeting the frequencies 0.1 - 10 Hz [1], naturally has this noise source. TOBA utilises torsion pendulums at high sensitivities to detect these gravitational fluctuations, which can be used for early earthquake detection [2] and sensing the gravitational waves from the mergers of intermediate mass black holes [1]. In this work, we study the suspension noise of torsion pendulums, and study how the use of two key technologies, cryogenic temperatures and crystalline fibres can reduce it.

To quantify the suspension thermal noise, we focus on measuring the Q factor, with which we can calculate the suspension thermal noise, given other parameters such as the temperature, and the relevant frequencies.

Method

A copper beryllium torsion pendulum with a sapphire suspension fibre was placed in a cryogenic chamber. The Q factor of the torsion pendulum was then measured via the ringdown method as the setup was thermally cycled from room temperature to 4 K and back. The radial position of the torsion pendulum was measured using an optical lever. The torsion pendulum was excited using coil-coil actuators, to allow for the ringdown measurement to take place.
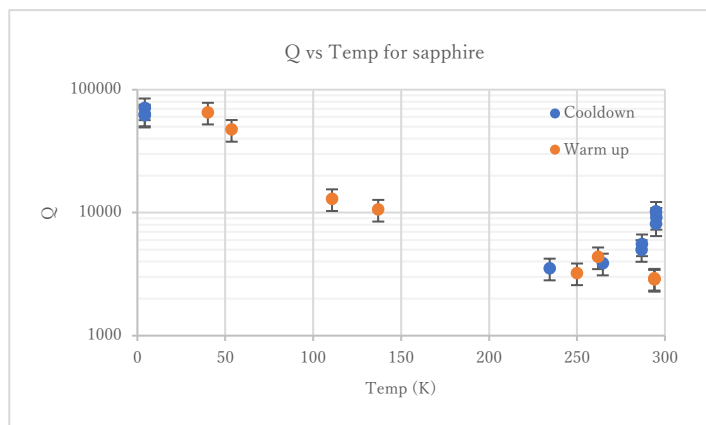

FIG 1. Graph of Q vs Temperature for a sapphire suspension fibre. The Q values ranged from 3 000 to 70 000 at 4 K, showing a great dependence on temperature, and follows the expectation that Q should increase at cryogenic temperatures. The resonance frequency was at 6 Hz, within the TOBA targeted frequencies of 0.1 – 10 Hz.

FIG 2. Picture of torsion pendulum, with attached mirror for optical lever readout, and coils for coil-coil actuation. The sapphire fibre used for suspension is 1 mm in diameter

Reference

[1]M. Ando *et al*., *Phys. Rev. Lett.*, 105, 161101 (2010)
[2]J. Harms *et al*., *Geophys. J. Int.*, 201, 1416-1425 (2015)

4th IFQMS

QUANTUM INNOVATION 2021

Angular Sensor with a Coupled Cavity for Gravity Gradient Sensing

Yuka Oshima[1], Satoru Takano[1], Ching Pin Ooi[1], Yuta Michimura[1], and Masaki Ando[1]

[1]*Department of Physics, University of Tokyo*

yuka.oshima@phys.s.u-tokyo.ac.jp

Introduction

TOrsion-Bar Antenna (TOBA) is a highly sensitive gravity gradient sensor using torsion pendulums [1]. The resonant frequency of torsional motion is ~1 mHz, therefore TOBA has good design sensitivity in low frequencies (0.1 – 10 Hz). A prototype detector Phase-III TOBA with a 35 cm-scale pendulum is under development to demonstrate noise reduction [2]. The target sensitivity is set to 10^{-15} /√Hz at 0.1 Hz. Phase-III TOBA can detect earthquakes with magnitude 7 or larger within 10 seconds from 100 km distance, therefore Phase-III TOBA is useful for gravity-based earthquake early warning [3]. To achieve our target sensitivity, we need to measure the pendulum rotation precisely. We propose a coupled wavefront sensor as an angular sensor for Phase-III TOBA. We show the principle and experimental demonstration status of a coupled wavefront sensor.

Method

For a conventional wavefront sensor, we build a linear cavity with two mirrors (FIG. 1. Top). When a mirror tilts, a part of the zero-order Hermite-Gaussian (HG) modes converts into the first-order HG modes. We detect it as angular signal. In the cavity, the first-order HG modes are anti-resonant since they get non-zero Gouy phase shift compared to the zero-order HG modes.

A coupled wavefront sensor is a new wavefront sensor using an optical coupled cavity. In our method, we put one more mirror behind a main cavity and build an auxiliary cavity (FIG. 1. Bottom). An auxiliary cavity can compensate Gouy phase of main cavity, therefore the zero-order and the first-order HG modes are resonant simultaneously. As a result, angular signal is enhanced in the main cavity.
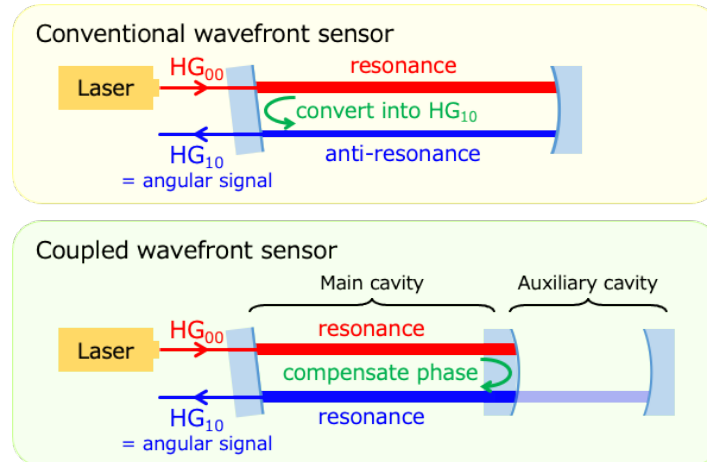

FIG. 1. Top: The schematic of a conventional wavefront sensor. Bottom: The schematic of a coupled wavefront sensor.

Acknowledgments

Reference

[1]M. Ando *et al.*, *Phys. Rev. Lett.*, 105, 161101 (2010).

[2]T. Shimoda *et al.*, *International Journal of Modern Physics D*, 29, 1940003 (2020).

[3]T. Shimoda, PhD thesis, The University of Tokyo (2019).

SE-03A-δ1-04

Towards sensitive accelerometers with levitated single nanoparticles

K. Aikawa[1], M. Kamba[1], H. Kiuchi[1], K. Okuda[1], N. Suyama[1], and R. Shimizu[1]

[1]*Department of Physics, School of Science, Tokyo Institute of Technology*

aikawa@phys.titech.ac.jp

Introduction

Single nanoparticles levitated in vacuum are a promising platform for sensitive accelerometers as well as for exploring macroscopic quantum physics. Cooling of their motion to the ground state of a trapping potential, corresponding to temperatures of about 10 μK, has recently been demonstrated. We plan to use levitated nanoparticles as sensitive accelerometers. For this purpose, we develop two experimental setups: one with an optical lattice, and one with an ion trap. In this presentation, we briefly introduce the latest results from both setups.

Method

In a setup with an optical lattice, we find that the phase noise of the trapping laser has a crucial impact on the motion along optical lattice. When the phase noise as well as the intensity noise are decreased, the center-of-mass motion along the optical lattice is cooled to near the ground state via electric feedback cooling[1]. The position sensitivity demonstrated in our setup is better than $10 \, \mathrm{fm}/\sqrt{\mathrm{Hz}}$, suggesting that nanoparticles is a promising system as a sensitive accelerometer.

In a setup with an ion trap, we design and fabricate a novel electrode geometry allowing us to place a high-numerical-aperture lens, required for observing the motion of nanoparticles, close to the electrodes. In this ion trap, we demonstrate the stable confinement of nanoparticles and observe their three-dimensional motion via the high-numerical-aperture lens. Due to the low oscillation frequency of nanoparticles in the ion trap, the ion-trap setup is also a promising setup for the sensitive detection of acceleration.

Reference

[1]M. Kamba, H. Kiuchi, T. Yotsuya, and K. Aikawa, *Phys. Rev. A* 103, L051701 (2021).

SE-03A-δ1-05

4th IFQMS

QUANTUM INNOVATION 2021

Interferometric gyroscope using slow and continuous atomic beam

Tomoya Sato[1], Ryotaro Inoue[1], Mikio Kozuma[2,1]

[1]Institute of Innovative Research, Tokyo Institute of Technology

[2]Department of Physics, School of Science, Tokyo Institute of Technology

sato@qnav.iir.titech.ac.jp

Introduction

A self-localization method, which does not rely on external signals, complements methods such as satellite positioning by the GPS signal, ensuring safety and improving estimation accuracy by hybridization. Such a method is also essential for navigation in environments where other methods cannot be applied, for example, under the sea.

One can estimate their position by integrating the angular velocity and acceleration in time. Such a self-localization method consists of a gyroscope and accelerometer is called inertial navigation. The accuracy of the current high-end inertial navigation system is dominated by the performance of the gyroscope, which employs the optical Sagnac effect, such as the ring laser gyroscope. The magnitude of the phase difference between counter-propagating waves for the Sagnac interferometer is inversely proportional to the product of wavelength and velocity of the wave. Thus, the matter-wave interferometer is a promising way to improve the phase sensitivity of the gyroscope since the wavelength and velocity of the matter-wave are much smaller than those of the light wave [1]. We aim to develop the matter-wave gyroscope utilized by the slow and continuous atomic beam interferometer, which can be mounted on a vehicle.

Method

A pair of atomic beams which is extracted from the 2D+MOT [2] is introduced into the interferometer region, where three pairs of counter-propagating Raman beams form the π/2-π-π/2 Mach-Zehnder type interferometer [3]. The Sagnac effect causes the sinusoidal variation between populations of internal states of the atom as a function of the angular velocity on the Sagnac loop. Thus, the rotation of the system can be deduced from the phase shift in the interference signal.

The measured phase shift reflects the rotation of the system, but at the same time, acceleration and environmental disturbances also change the phase. It is necessary to eliminate these effects for accurate measurement. It can be achieved by using a pair of atomic interferometers with atomic beams that share Raman lights and travel in opposite directions [4]. Since the sign of phase shift induced by the rotation depends on the velocity vector, but that induced by the spurious effect is not. By measuring the differential phase shift between two interferometers, we can extract the phase shift caused by rotation while eliminating that caused by common-mode noises.

We measured the phase shift in the interference signal as a function of the tilting angle of the optical table on which the apparatus was installed (FIG.1). The linear phase shift due to the gravitational acceleration was observed as a function of the tilting angle. It was also confirmed that the common-mode rejection reduced that linear phase shift. The remaining phase shift after the rejection was consistent with the shift caused by the angular velocity of the Earth's rotation. To the best of our knowledge, this is the first demonstration of a gyroscope using the slow and continuous atomic beam.
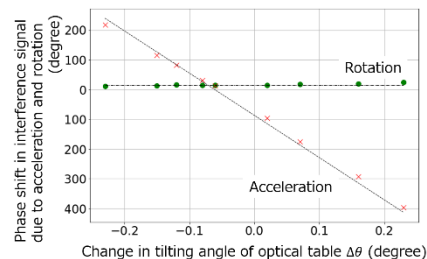

FIG. 1 Phase shift in interferometer due to the acceleration and rotation. Dashed lines indicate theoretical values.

Reference

[1]J. F. Clauser, *Physica B*, <u>151</u>, 262 (1988).

[2]K. Dieckmann, R. J. C. Spreeuw, M. Weidemüller, and J. T. M. Walraven, *Phys. Rev. A*, <u>58</u>, 3891 (1998).

[3]M. Kasevich and S. Chu, *Phys. Rev. Lett*, <u>67</u>, 181 (1991).

[4]T. L. Gustavson, P. Bouyer and M. A. Kasevich, *Phys. Rev. Lett*, <u>78</u>, 2046 (1997).

SE-03A-δ1-06

Development of a quantum gyroscope based on a single ion trapping techniques

Ryoichi Saito[1,2], and Takashi Mukaiyama[1,2]

[1] Graduate school of Engineering, Osaka University

[2]QIOB, Osaka University

r_saito@ee.es.osaka-u.ac.jp

Introduction

  Atoms in a coherent superposition of different momentum states enable high-precision measurement of physical quantities. Matter-wave interferometers typically exploit entanglement between the internal state and the motional state of matter. The accumulated matter-wave phases for different paths are obtained from the interference signal of the internal states after the closing pulse of the interferometer. In order to achieve precise sensing, exquisite control of internal and external states of individual quanta is essential. Atoms and ions are ideal matter for such use since they provide us with the precise control of their quantum states using optical means. So far, neutral atoms have been used for various sensing applications such as detection of gravitational acceleration[1], electric and magnetic field[2], rotation[3] and so on. On the other hand, a trapped ion has not been considered for a platform to realize sensing of external perturbations until recently. This may partly be because of the difficulty in realizing a large interference area due to the tight confinement of the ion trap, which is inextricably linked with the advantage of a capability of stable trapping. Quite recently, Campbell and Hamilton proposed to utilize a trapped ion for a precise rotation sensing application. In the proposal, a trapped ion in a circular motion constructs a Sagnac interferometer. By taking an arbitrary number of ion rotations, the sensitivity of the rotation sensing can be tuned, and the ions with multiple circular motions may provide us with a large interference area and a compact physical size at the same time.

Method

   The Sagnac interferometer, which utilizes the single trapped ion, is realized by circularly propagating wave packet of the ion. The protocol to generate the two-dimensional circular interferometer is as below. First, we apply the microwave half pi pulse to the ion in a two-dimensional isotropic potential for creating the superposition of the internal spin state. Then, we irradiate a mode-locked laser at 355 nm to apply the momentum kick, depending on the internal spin state, to generate the one-dimensional interferometer[5]. After the generating spin-motion entangled state by spin-dependent momentum kick, non-adiabatic trap potential shift in a perpendicular direction to the momentum kick is applied by step voltage to the electrode[6]. Then, the wave packet of the ion propagates an elliptical orbit. The rotation of the system produces the path difference between clockwise and counterclockwise. The phase shift of the ion matter-wave due to the rotation is measured by the detection probability of the internal state.

   In the presentation, we will talk about our experimental detail and the current achievement.

FIG. 1. Schematic diagram of rotation sensing using a trapped ion

Reference

[1]M. Kasevich and S. Chu, *Phys. Rev. Lett*. 67, 181 (1991).

[2]K. Zeiske, G. Zinner, F. Riehle, and J. Helmcke, *Appl. Phys. B* 60, 205 (1995).

[3]T. L. Gustavson, P. Bouyer, and M. A. Kasevich, *Phys. Rev. Lett*. 78, 2046 (1997).

[4]W. C. Campbell and P. Hamilton, *J. Phys. B: At. Mol. Opt. Phys.* 40

[5]A. Shinjo, M. Baba, K. Higashiyama, R. Saito, and T. Mukaiyama, *Phys. Rev. Lett.* 126, 153604 (2021).

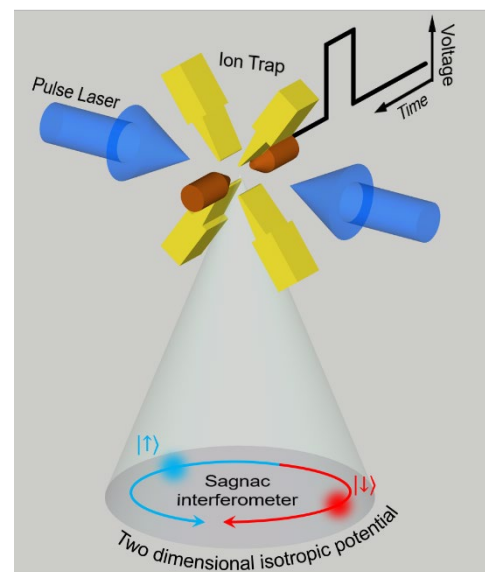[6] R. Saito and T. Mukaiyama, *Phys. Rev. A* 104, 053114 (2021)..

Exponentially Enhanced Quantum Metrology by Quenching Superradiant Light-Matter Systems Beyond the Critical Point

Karol Gietka, Lewis Ruks, and Thomas Busch

Okinawa Institute of Science and Technology, Quantum Systems Unit

Karol.Gietka@oist.jp

Introduction

We present a quantum metrology protocol which relies on quenching a light-matter system exhibiting a superradiant quantum phase transition beyond its critical point. In the thermodynamic limit these systems can exhibit an exponential divergence of the quantum Fisher information in time, whose origin is the exponential growth of the number of correlated photons on an arbitrarily fast time scale determined by the coupling strength. This provides an exponential speed-up in the growth of the quantum Fisher information over existing critical quantum metrology protocols observing power law behavior. We demonstrate that the Cramer-Rao bound can be saturated in our protocol through the standard homodyne detection scheme. We explicitly show its advantage in the archetypal setting of the Dicke model and explore a quantum gas coupled to a single-mode cavity field as a potential platform. In this case an additional exponential enhancement of the quantum Fisher information can in practice be observed with the number of atoms N in the cavity, despite existing works suggesting a requirement of N-body coupling terms.

Reference

K. Gietka, L. Ruks, T. Busch, *arXiv*, S. Schmitt, *Science*, 2110:04048, (2021).

4th IFQMS

QUANTUM INNOVATION 2021

Three-layered Magnetically Shielded Room for Ultrahigh-sensitivity Quantum Sensing of Biomagnetic Signals

Motofumi Fushimi[1], Akihiro Kuwahata[2], Shinichi Chikaki[1],

Takao Yamaguchi[3], Yuuki Niwa[3], and Masaki Sekino[1]

[1]*Graduate School of Engineering, The University of Tokyo*

[2]*Graduate School of Engineering, Tohoku University*

[3]*Ishida Ironwork's Co., Ltd.*

motofumi-fushimi@g.ecc.u-tokyo.ac.jp

Introduction

Measurement of biomagnetic fields generated from biological tissues such as the brain and heart has attracted great attention since it enables us to observe physiological activities of living organisms. Quantum sensers such as the optically pumped atomic magnetometer and the nitrogen-vacancy center in diamond have achieved ultrahigh-sensitivity sensing of magnetic fields and opened the field of biomagnetic signal sensing at room temparature. However, to measure the extremely weak biomagnetic signals (typically at the order of picotesla), a magnetically shielded room (MSR) that prevents the ambient magnetic field (typically at the order of microtesla) from contaminating the target biomagnetic signals is essential [1].

In this study, we developed an MSR made of three-layered permalloy plates and measured its shielding factor to validate the efficacy of the shield in biomagnetic sensing such as magnetoencephalography (MEG) of small animals.

Methods

Figure 1 shows the developed MSR consisting of three layers of permalloy plates and one layer of aluminum plate for shielding high frequency fields. The inside dimension of the MSR is 3 m x 2 m x 2 m, and thus available for wide range of biomedical applications including human subjects. For the measurement of the magnetic fields, we used a highly sensitive fluxgate sensor (502A, APPLIED PHYSICS SYSTEMS). While applying the external AC magnetic fields at 0.1-100 Hz, we evaluated the shielding factor defined here as the ratio of magnetic field strength inside to outside the MSR.

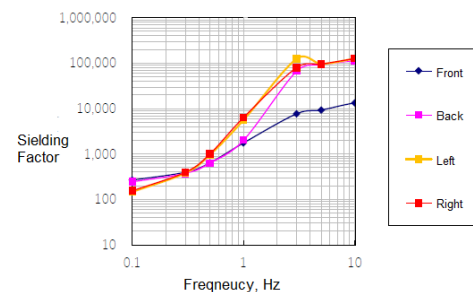FIG. 1. Three-layered MSR developed in this study.

FIG. 2. The shielding factor at each four side of the MSR

Results and Discussion

Figure 2 shows the shielding factor of four each side of the MSR. The shielding factor increases with frequency thanks to the aluminum layer and the factor of about 10^4-10^5 is achieved at 10 Hz, which corresponds to the frequency of the alpha wave of humans. The shielding factor measured at the front side is relatively low. This is because the door of the shield deteriorates the effect of the aluminum layer. Although the MSR greatly suppresses the magnetic field, an additional shielding factor of about 10^2 is required to achieve the sensing of picotesla-scale biomagnetic signals. Introducing an active cancelling coil in the MSR would provide the sufficient shielding capability [2,3], evaluation of which is our future work.

Acknowledgements

References

[1]T. J. Sumner *et al.*, *J. Phys. D: Appl. Phys.*, 20, 1095 (1987).
[2]K. Harakawa *et al.*, *IEEE Trans. Mag.*, 32(6), 5256-5260 (1996).
[3]E. Boto *et al.*, *Nature*, 555, 657-661 (2018).

Super-resolution in nano-NMR

Nicolas Staudenmaier[1, *], Santiago Oviedo-Casado[2], Anjusha Vijayakumar-Sreeja[1], Genko Genov[1], Alex Retzker[2] and Fedor Jelezko[1,4]

[1]Institute for Quantum Optics, Ulm University, D-89081 Ulm, Germany

[2]Racah Institute of Physics, The Hebrew University of Jerusalem, Jerusalem 91904, Givat Ram, Israel

[4]Center for Integrated Quantum Science and Technology, Ulm University, D-89081 Ulm, Germany

*nicolas.staudenmaier@uni-ulm.de

Introduction

There is increasing interest in reducing the size of NMR and MRI devices to gain new insights to processes on the nanoscale. These include for example NMR studies of single cells, neurons[1], or surfaces and surface chemistry[2]. Nitrogen-vacancy (NV) centers in diamond show to be promising sensors for such applications. In the past years nano- to microscale NMR has been proven using single[3, 4] or ensemble NV centers[5]. Importantly, unlike in conventional NMR, signal pickup with NV centers does not depend on the strength of an applied external magnetic field, allowing for the acquisition of information-rich spectra from zero and low-field[6] as well as high-field NMR. On the other side nanoscale NMR resorts to statistical nuclear spin polarization rather than directional such as thermal polarization. For that reason, spectral resolution is limited by diffusion of a liquid sample in the detection volume. However, there is theoretical evidence that the signal correlation does not drop off exponentially but that there is a polynomial tail for longer times allowing a sharp peaked signal in the spectrum[7, 8]. We will show experimental evidence that promotes such a model that overcomes any resolution limit and ultimately enables super-resolution of signals with nearby frequencies.

Method

Experimental measurements are done on a homebuilt confocal microscope using single shallow NV centers located about 10nm below the diamond surface. Hydrogen nuclear spins, naturally present in the used immersion oil, are sensed via a nuclear spin sensitive dynamical decoupling sequence in combination with the quantum heterodyne (Qdyne) measurement protocol[9], that correlates all individual readouts. From the data the autocorrelation of the NMR signal is obtained and analyzed using different statistical tools.

References

[1] M. Grisi et al., *Sci. reports* **7**, 44670 (2017).
[2] G. A. Somorjai and Y. Li, *Proc. Natl. Acad. Sci.* **108**, 917–924 (2011).
[3] H. J. Mamin et al., *Science* **339**, 557-560 (2013).
[4] T. Staudacher et al., *Science* **339**, 561-563 (2013).
[5] D. Glenn et al., *Nature* **555**, 351–354 (2018).
[6] M. Ledbetter et al., *J. Magn. Reson* **199**, 25-29 (2009)*.
[7] D. Cohen et al., *Sci. Rep.* **10**, 5298 (2020).
[8] S. Oviedo-Casado et al., *Sci. Rep.* **10**, 19691 (2020).
[9] S. Schmitt et al., *Science* **356**, 832-837 (2017).

Sensitivity of weight imaging using a hybrid system based on piezoactive magnetic material and diamond quantum sensor

Ryota Kitagawa[1], Shunsuke Nagata[1], Soki Urashita[1], Keigo Arai[1,2], Kosuke Mizuno[1],

Hitoshi Ishiwata[1,2], Yota Takamura[1],

Takayuki Iwasaki[1], Shigeki Nakagawa[1], and Mutsuko Hatano[1]

[1]*Department of Electrical and Electronics Engineering, School of Engineering, Tokyo Institute of Technology*
[2]*PRESTO, Japan Science and Technology Agency*
kitagawa.r.ab@m.titech.ac.jp

Introduction

Imaging weight over multiple length scales from single cells to biological tissues, remaining a key challenge, introduces a new modality for studying biological systems. Such a high dynamic range in length scale can be realized by a hybrid sensor based on magnetostrictive(MS) magnetic material [3] and nitrogen-vacancy (NV) centers in diamonds [4]. To detect the weight of human egg cells, the weight accuracy of ~ 1 Pa is required. In this research, we evaluated the weight sensitivity of the hybrid system. We measured weight-to-magnetic field conversion efficiency and magnetic field sensitivity.

Method

We fabricated a hybrid sensor by gluing a MS magnetic material of a $SmFe_2$ thin film[3], deposited on an ultra-thin quartz substrate, and NV centers in a diamond film deposited on a type-Ib diamond (111) substrate (Fig. (a))[5]. Various weight was applied through a rivet in an area of 3.1 mm^2 by changing the number of calibrated weights (0 ~125 kPa). Due to the inverse MS effect, weight is converted into the rotation of magnetization in the MS layer (Fig. (b)). This rotation induces a change in the stray magnetic field, imaged by NV centers via optically-detected magnetic resonance (ODMR). We imaged the magnetic field by continuous-wave ODMR while changing the weight. One pixel of the image is $(4.9 \ \mu m)^2$.

Result

Fig. (c) shows a magnetic field image at 0 kPa. We successfully imaged the magnetic field from $SmFe_2$. Fig. (d) shows the Bz-pressure dependence of one pixel. Weight-to-magnetic field conversion efficiency was 70 nT/kPa. The estimation accuracy of Bz was about 2 μT per one pixel. Thus, the estimation accuracy of weight was 28 kPa. Depositing $SmFe_2$ on the NV center will improve the conversion efficiency by an order. Further improvement of magnetic field sensitivity is required, such as utilizing pulsed measurement, improvement of coherence time and generation rate of NV center, and spatial integration of the ODMR signal.

Reference

[1] G. Popescu et al., Lab Chip **14**, 646-652 (2014).
[2] D. Martínez-Martín et al., Nature **550**, 500-505 (2017)
[3] Y. Takamura, et al.,2019 Annu. Conf. on MMM, Las Vegas, AQ-11,5 Nov. 2019.
[4] J. Cai et al., Nat. Commun. **5**, 1 (2014).
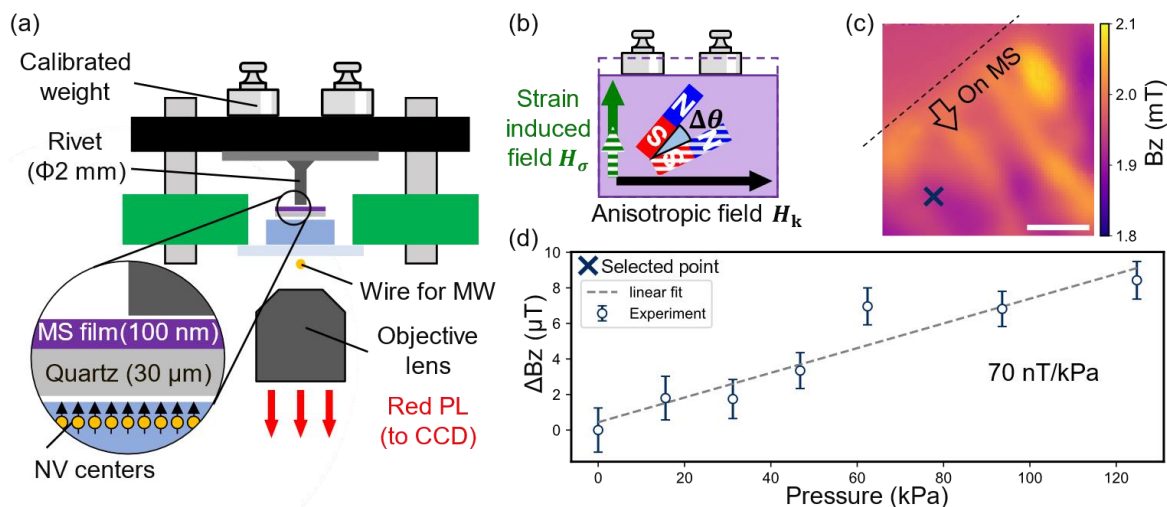[5] K.Tahara et al., Appl. Phys. Lett. **107**, 193110 (2015)

Fig. (a) Setup of hybrid weight imaging system. (b) Weight-dependent rotation of magnetization due to inverse MS effect. (c) Magnetic field image at 0 kPa. The upper light area is off MS film. The scale bar is 100 μm. (d) Bz-pressure dependence of a selected point. Error bar is the $\pm 1.96\sigma$ confidence interval. Weight-to-magnetic field conversion efficiency was 70 nT/kPa.

Study on electron spin control method for high-sensitivity diamond quantum sensor

Hiroyoshi Tomioka[1], Yuji Hatano[1], Takeharu Sekiguchi[1], Keigo Arai[1], Hiromitsu Kato[2],

Shinobu Onoda[3], Takeshi Ohsima[3], Takayuki Iwasaki[1], and Mutsuko Hatano[1]

[1]*Department of Electrical and Electronics Engineering, School of Engineering, Tokyo Institute of Technology*

[2] *National Institute of Advanced Industrial Science and Technology*

[3]*National Institutes for Quantum and Radiological Science and Technology*

tomioka.h.ac@m.titech.ac.jp

Introduction

A diamond quantum sensor utilizing the NV center, a paramagnetic defect composed of nitrogen and vacancy in diamond, is expected to be applied to life-science [1] and automotive fields due to its high sensitivity and room temperature operation. However, further improvements in DC-field sensitivity and miniaturization are demanded for practical applications. To achieve such improvements, we focus on CE (continuously excited)-Ramsey method [2] as an alternative to the conventional method of continuous-wave optically detected magnetic resonance (CW-ODMR) or regular Ramsey.

Methods

In CE-Ramsey measurement, the excitation light is continuously applied while the microwaves are pulsed to control the electron spin states. Our experimental setup is shown in Fig. 1(a). In this study, we performed CW-ODMR, CE-SQ (single quantum)-Ramsey, and CE-DQ (double quantum)-Ramsey measurements to compare the magnetic sensitivities between them. We also estimated the shot noise limited sensitivities of CW-ODMR and CE-SQ-Ramsey methods. For this calculation, we solved the rate equations involving only five levels [3]: two ground states, two excited states, and a metastable state. The diamond sample used was grown by CVD (100 μm thickness) using ^{12}C-enriched methane on a IIa substrate with a (111) surface, followed by electron beam irradiation ($5 \times 10^{17} \mathrm{cm}^{-2}$) and annealing.

Results and discussion

The magnetic sensitivities obtained by CW-ODMR, CE-SQ-Ramsey, and CE-DQ-Ramsey methods are plotted in Fig. 1(b). The CE-SQ-Ramsey and CE-DQ-Ramsey measurements showed better magnetic sensitivities than CW-ODMR for the modulation frequency between 10 and 90 kHz. Fig. 1(c) shows the calculation result of the shot noise limited sensitivity. This sensitivity is better for CE-SQ-Ramsey than CW-ODMR at high modulation frequencies (above 20 kHz). In addition to the sensitivity improvement, CE-Ramsey is suitable for miniaturization because it does not require pulsing of a high-power laser, which is essential for the regular Ramsey. Therefore, we expect it to be used for applications such as battery monitoring in electric vehicles.

Reference

[1] J. F. Barry *et al.*, Proc. Natl. Acad. Sci. USA, **113**, 14133 (2016).   [2] C. Zhang *et al.*, Phys. Rev. Appl. **15**, 064075(2021).
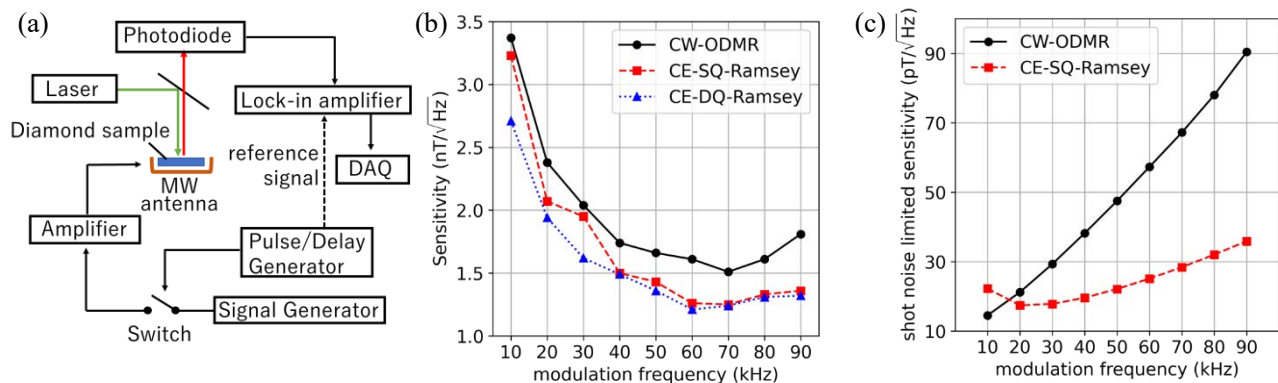[3] K. Jensen *et al.*, Phys. Rev. B **87**, 014115 (2013).

FIG. 1. (a) Schematic of the experimental setup. (b) Comparison of the experimental magnetic sensitivities with different modulation frequencies. (c) Comparison of the shot noise limited sensitivities calculated by using five level model with different modulation frequencies.

4th IFQMS   QUANTUM INNOVATION 2021

Optically detected magnetic resonance spectra of silicon vacancies in 4H-SiC with different temperatures

S. Motoki[1,2], S.-I. Sato[2], Y. Masuyama[2], Y. Yamazaki[2], Y. Hijikata[1], T. Ohshima[2]

[1] [1]*Science and Engineering, Course in Electrical and Electronic Systems, Saitama University*

[2]*National Institutes for Quantum Science and Technology*

E-mail: s.motoki.639@ms.saitama-u.ac.jp

Introduction

Silicon vacancy (V_{Si}^-) centers in silicon carbide have attracted attention because of their potential applications to quantum sensors (high-sensitivity magnetic field and temperature sensors). V_{Si}^- centers are also expected to be used for magnetic sensors under harsh environments such as space and undergrounds, since they have structural stability and the potential of high-fidelity spin manipulation at high temperatures[1]. To realize V_{Si}^- based magnetic sensors operating at high temperature, understanding of optically detected magnetic resonance (ODMR) in the ground states of V_{Si}^- centers, which is the basic principle of magnetic sensing, is crucial. In particular, the effects of temperature on the ODMR spectra are less well understood. Here, we demonstrate the potential of V_{Si}^- magnetic sensors at high temperatures by showing the ODMR spectra with different temperatures. We also systematically investigate the effects of high energy electron irradiations on the ODMR spectra of formed V_{Si}^- centers. The concentration of V_{Si}^- centers increases with increasing electron irradiation dose, resulting in the enhancement of sensitivity, but increase in undesired defects which can cause decoherence is also expected. Hence, the effects of electron irradiation dose should be clarified to obtain better sensitivity of V_{Si}^- based magnetic sensors.

Method

High purity semi-insulating (HPSI) 4H-SiC was irradiated with 2 MeV electrons at room temperature up to the dose of 3×10^{18} cm^{-2} to form V_{Si}^- centers. The samples were then thermally annealed at 873 K for 30 minutes in vacuum to obtain stability during measurements at high temperature. FIG. 1 shows ODMR spectra of V_{Si}^- centers in 4H-SiC at different temperatures. The 785 nm laser at 40 mW was used for excitation and the emitted photons above 900 nm were collected by an InGaAs photo detector. Under zero magnetic field, a resonant peak at 70 MHz due to zero-field splitting of V_{Si}^- ground states appeared even at 600 K, being reduced with increase temperature. The resonant peak was split into two peaks by applying external magnetic field (Zeeman splitting). These results suggest that spin manipulation of V_{Si}^- centers is possible at 600 K and thus high temperature operation of V_{Si}^- based magnetic sensor is feasible. At the presentation, the mechanism of change in ODMR spectra with different temperatures is discussed. In addition, the relationship between the ODMR spectra and the electron irradiation dose is reported.
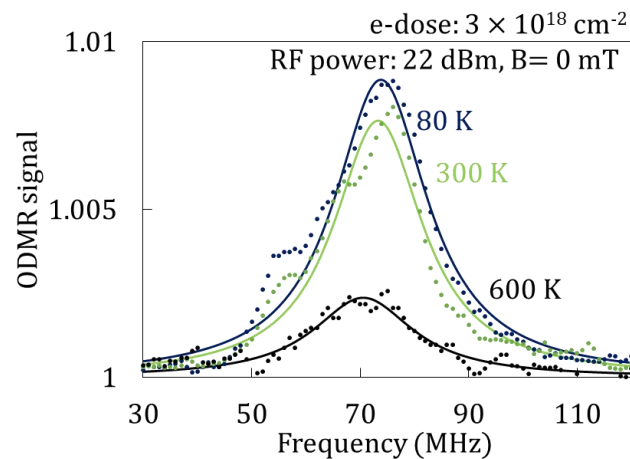
FIG. 1. ODMR spectra of V_{Si}^- centers in 4H-SiC at different temperatures. Experimental data (symbols) are fitted by the Lorentzian function (solid lines).

Reference

[1] H. Kraus et al., Sci. Rep. **4**: 5303 (2014).

SE-03A-α2-06

High efficiency formation of NV center inside diamond by femtosecond laser

Ryusei Yanoshita[1], Torataro Kurita[1], Yasuhiko Shimotsuma[1],
Masanori Fujiwara[2], Norikazu Mizuochi[2], Masahiro Shimizu[1], Kiyotaka Miura[1]
[1]Department of Material Chemistry, School of Engineering, Kyoto University
[2]Institute for Chemical Research, Kyoto University
yanoshita.ryuusei.66a@st.kyoto-u.ac.jp

Introduction

The ensemble of NV centers, consisting of impurity nitrogen and adjacent vacancies in diamond, are expected as quantum sensors due to their long coherence time and possible coherent control of a single spin at room temperature [1]. Although the single NV center formation by femtosecond laser irradiation has been reported [2], the formation mechanism is not fully understood. Especially, the transformation of diamond to graphite [3] and the effective laser irradiation parameters for the formation of NV center ensemble remain unexplored. More recently, we have demonstrated that the pulse width and the number of pulses are effective to generate a higher density NV center ensemble [4, 5]. Here we report on the relation between the impurity nitrogen concentration and the laser irradiation parameters for the NV center formation. In particular, we focused on the efficiency of the NV center formed by the femtosecond laser irradiation with different pulse repetition rates.

Method

A femtosecond laser beam with a central wave length of 800 nm (bandwidth 37 nm) and a pulse width of 60 fs was focused in a diamond sample through the objective lens (50× NA 0.80). The focus was located at a depth of 50 μm below the sample surface. In the experiments, two diamonds with different nitrogen concentrations (Sample A: CVD synthesized Type IIa diamond, [N] ≤ 1 ppm, Sample B: HPHT synthesized Type Ib diamond, [N] ≈ 33 ppm) were used. The laser pulses were irradiated from the normal to the (100) plane. To reveal the effect of the impurity nitrogen concentration, the PL intensity originated from the NV- center ranging from 640 nm to 660 nm between the different diamond samples was compared. Since the threshold of NV center formation by the femtosecond laser irradiation depends on the impurity nitrogen concentration, we tuned the pulse energy (E_p) according to the samples. The E_p between 50 nJ and 200 nJ was applied for sample A, on the other hand, the E_p was set to 2000 nJ for sample B. Other laser parameters such as the pulse width (60 fs), pulse repetition rate (250 kHz), and the number of pulses (2.5×10^5) were set the same. Table 1 shows the PL intensity (I_{PL}) normalized by that in the unirradiated region. Despite the fact that the E_p for sample A was lower than that for sample B in all experiments, the PL intensity for sample A reached approximately 4.4 times higher than that for sample B. Assuming the PL intensity is proportional to the NV center concentration, this result indicates that the formation efficiency for the NV center is high when the impurity nitrogen concentration is low. We have also confirmed the formation efficiency of the NV center by the femtosecond laser irradiation with various pulse repetition rates ranging from 5 kHz to 250 kHz. In the laser experiments, the irradiated number of pulses was set to be 2.5×10^5 pulses by changing the irradiation time. Fig. 2 shows the normalized PL intensity was changed by the pulse repetition rate, despite that the same total pulse energy was irradiated. In particular, the NV center concentration decreased at 10 kHz or less and 100 kHz or more. In the case below 10 kHz, corresponding to the pulse interval of 100 μs, such timescale is quite longer than that for thermalization and the lifetime of the exciton in diamond (~ 1 μs). Furthermore, the decrease of NV center concentration at 100 kHz or more could be interpreted in terms of the annihilation of NV center or the transformation into the different defects such as H3 center.

Table1. Normalized PL intensity of NV center in two different types of diamonds.

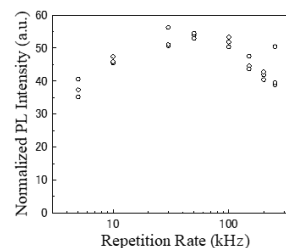| Type	E_p [nJ]	I_{PL}
Ib	2000	8.21
IIa	50	4.05
IIa	100	17.4
IIa	200	35.8

Fig. 2. Normalized PL intensity of NV center induced by the femtosecond laser pulses with various pulse repetition rates.

Reference
[1] A. Gruber, et al., *Science* 276 2012 (1997).
[2] Y. Chen, et al., *Nat. Photonics* 11 77 (2017).
[3] M. Sakakura, et al., *J. Laser Micro/Nanoeng.* 11 346 (2016).
[4] T. Kurita, et al., *Appl. Phys. Lett.* 113 211102 (2018).
[5] T. Kurita, et al., *Appl. Phys. Lett.* 118 214001 (2021).

AC magnetic field sensing with ensemble NV centers using electrical detection methods

Hiroki Morishita[1], Naoya Morioka[1], Tetsuri Nishikawa[1], Hajime Yao[1], Shinobu Onoda[2],

Hiroshi Abe[2], Takeshi Ohshima[2], and Norikazu Mizuochi[1]

[1]*Institute for Chemical Research, Kyoto University, Uji, Kyoto 611-0011, Japan.*

[2] *National Institutes for Quantum and Radiological Science and Technology, Takasaki, Gunma, 370-1292, Japan.*

h-mori@scl.kyoto-u.ac.jp

Introduction

Nitrogen-vacancy (NV) centers in diamond have a long coherence time at room temperature, and hence they are candidates for quantum sensors and quantum information processing devices [1]. While electrical detection of NV spins is essential to develop and integrate these quantum devices [2-8], to the best of our knowledge, there are no demonstrations of AC magnetic field sensing using electrical detection methods. In the electrical detection of the NV spins, the change in the photocurrent is measured when resonant microwaves are applied to the NV spins. In the demonstration of the AC magnetic field sensing using electrical detection methods, the current generated by the AC magnetic field flows in the diamond sample. This current generated by the AC magnetic field can cause an increase in noise in the electrical detection method. Thus, the AC magnetic field sensing using the electrical detection method is still challenging. In this study, we demonstrate for the first time AC magnetic field sensing using the electrical detection method by reducing the influence of such a current.

Method & Results

In this study, we performed the AC magnetic field sensing with an electrical detection method using the ensemble of NV centers (concentration of ∼ 1.4×10^{17} cm^{-3}) created by electron-beam irradiation followed by annealing. Figure 1 shows a result of AC magnetic field sensing with the electrical detection method with the bias voltage of 5 V. The result indicates that we observe ∼ 3×10^{-8} T/√Hz of the sensitivity of the AC magnetic field. In this presentation, we discuss the results of AC magnetic field sensing using the electrical detection method.
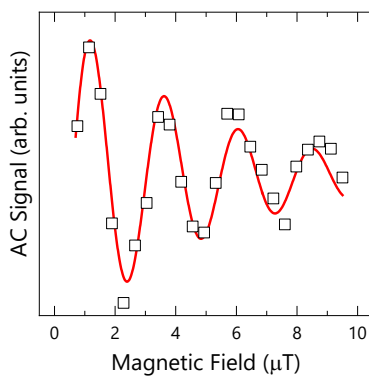

Fig.1 AC magnetic field sensing with an electrical detection method.

Acknowledgments

References

[1] E. D. Herbschleb et al., *Nat. Commun.* 10, 3766 (2019).
[2] E. Bourgeois et al., *Nat. Commun.* 6, 8577 (2015).
[3] F. M. Hrubesch et al., *Phys. Rev. Lett.* 118, 037601 (2017).
[4] M. Gulka et al., *Phys. Rev. Applied* 7, 044032 (2017).
[5] P. Siyushev, et al. *Science* 363, 728 (2019).
[6] H. Morishita et al., *Sci. Rep.* 10, 792 (2020).
[7] T. Murooka et al., *App. Phys. Lett.* 118, 253502 (2021).
[8] M. Gulka et al., *Nat. Commun*, 12, 4421 (2021).

4th IFQMS

QUANTUM INNOVATION 2021

OPuS-MAGNM - Miniaturized Optically Pumped Solid State Quantum Magnetometers for Space Applications

Hannes Kraus[1], Corey J. Cochrane[1]

[1]NASA Jet Propulsion Laboratory, California Institute of Technology, Pasadena, California, USA

hannes.kraus@jpl.nasa.gov

The OPuS-MAGNM project proposes to develop a novel low-cost low-power rad-hard miniaturized solid-state magnetometer for planetary magnetic field sensing. This technology leverages optically active, spin-carrying quantum centers (QC) in wide-bandgap semiconductors such as diamond or silicon carbide. External magnetic fields cause changes in the QC spin energy conformation, which can be detected optically. Wide-bandgap solid-state systems, in comparison to gas-cell based optically pumped magnetometers are interesting because of the material's intrinsic extensive temperature range (QC deterioration starts above Venus surface temperatures, at about 700C), and radiation hardness (QC implantation fluence $\sim10^{17}$ e/cm2 vs. Europa orbit 30 day fluence $\sim10^{13}$ e/cm2). Additionally, the sensor lends itself to miniaturization, as QC are sensitive down to single emitters, i.e. small, sub-mm ensembles are sufficient sensor volumes.

The U.S. Planetary Science Decadal Survey identifies the need for a number of scientific instruments addressing the three crosscutting themes of planetary science: (1) understanding solar system beginnings, (2) searching for the requirements for life and (3) revealing planetary processes. Magnetometers are unassuming, but powerful tools aiding in all of these themes.

The proposed technology is an extension to the recent Silicon Carbide solid-state magnetometer (SiCMAG[1]), adding substantially better sensitivities at the expense of requiring optical readout[2]. We leverage optical readout noise being shot noise in nature, while all-electrical systems suffer from 1/f noise. This gives the optical readout approach a significant advantage in low-frequency and long-term stability performance metrics.

Consider the two most commonly used magnetometer technologies flown in space: Fluxgate systems exhibit high sensitivities and all- electrical simplicity, but require multiple coils per spatial direction. Additionally, fluxgates are not self-calibrating; drifts in absolute field values necessitate either augmenting the fluxgate system with a self-calibrating system or incorporating complicated spacecraft roll maneuvers into mission planning.

Optically pumped He cell systems can counter this issue, operating both in scalar and vector mode, also with very high sensitivities. Their downside is the added complexity of the gas cell, with Helium being notoriously prone to outgas. Also, vector-helium systems are larger and more expensive than fluxgates. OPuS-MAGNM now marries the solid-state simplicity of fluxgates and SiCMAG with the precision and self-calibration capabilities of an atomic gas magnetometer system, with improving longevity over gas cells. It has the potential to provide self-calibrated, heritage-level vector magnetic field science in a radiation-hard and thermal/vacuum-rugged miniaturized package; well suited for all kinds of planetary science missions.
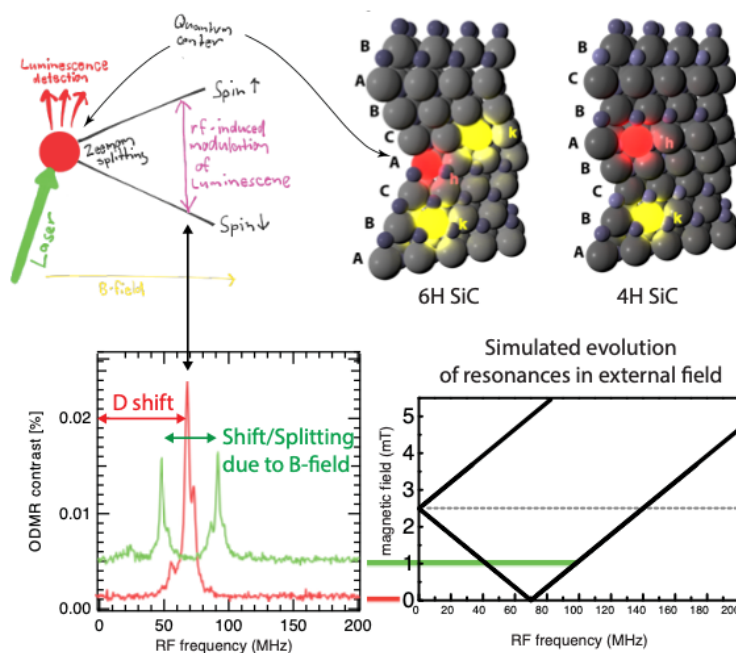

FIG. 1. Illustration of the signal genesis of the optically detected magnetic resonance (ODMR) in wide-bandgap solid-state semiconductors. Silicon vacancies in Silicon Carbide (h,k) are optically. active spin carrying quantum centers, addressable by resonant excitation of electronic and radio frequency transitions. An exemplary ODMR spectrum at zero magnetic field and 1mT field ist shown at the bottom left. A calculation of the resonance positions depending on the magnetic field is shown on the bottom right.[3]

References

1. C.J. Cochrane, J. Blacksberg, M.A. Anders, P.M. Lenahan. Vectorized magnetometer for space applications using electrical readout of atomic scale defects in silicon carbide. *Sci. Rep.* 2016, 6 (1), 1239.
2. H. Zheng, J. Xu, G.Z. Iwata, et al. Zero-Field Magnetometry Based on Nitrogen-Vacancy Ensembles in Diamond. *Phys. Rev. Applied* 2019, 11 (6), 064068.
3. H. Kraus, V.A. Soltamov, F. Fuchs, et al. Magnetic field and temperature sensing with atomic-scale spin defects in silicon carbide. *Sci. Rep.* 2014, 4, 5303.

4th IFQMS

QUANTUM INNOVATION 2021

Development of phthalocyanine ion beam for creation of multiple NV centers

Kosuke Kimura[1,2], Shinobu Onoda[1], Keisuke yamada[1], Wataru Kada[2], Tokuyuki Teraji[3],

Junichi Isoya[4], Osamu Hanaizumi[2], and Takeshi Ohshima[1]

[1] *National Institutes for Quantum Science and Technology*

[2] *Graduate School of Science and Technology, Gunma University*

[3] *National Institute for Materials Science*

[4] *Faculty of Pure and Applied Sciences, University of Tsukuba*

t201d208@gunma-u.ac.jp, kimura.kosuke@qst.go.jp

Introduction

A nitrogen vacancy (NV center in diamond is known as a solid-state spin qubit worked at room temperature. NV centers coherently coupled by dipole-dipole interactions have a potential to accomplish quantum registers operatable at room temperature. Since the dipole-dipole interaction is inversely proportional to the cube of the distance between the NV centers, it is necessary to create NV centers in close proximity to each other. One of the methods to create NV centers in close proximity is nitrogen (N ion implantation via a nanohole mask [1]. This method has been reported to create double coupled NV centers. However, for reason of nanohole purification technology, it has been difficult to create multiple coupled NV centers with this method. The other method is molecular ion implantation [2,3]. In 2013, *Yamamoto et al.* reported the dipolar coupled NV center pair via nitrogen molecular ion (N_2^+ implantation [2]. In 2019, *Haruyama et al.* reported the implantation of molecular ion from an adenine ($C_5N_5H_5$ ion source and demonstrated to create triple coupled NV centers [3]. It is expected to create further multiple coupled NV center by implantation of molecular ion with a higher number of nitrogen atoms than $C_5N_5H_5$. In this study, we report to develop a phthalocyanine($C_{32}N_8H_{18}$ ion beam containing eight nitrogen atoms for creation of multiple NV centers.

Method and result

The $C_{32}N_8H_{18}$ ion beam was developed using an ion implanter. Firstly, $C_{32}N_8H_{18}$ powder was vaporized and ionized by a heater at 336°C in the support gas (Ar ambient. Secondly, positive ions were electrically extracted by energy of 3 keV. Thirdly, the extracted beam was analyzed by mass spectrometry. The result of mass spectra was showed FIG. 1. The fragments, such as C_6H_4, C_8H_4, $C_8N_2H_5$, etc., and Ar were detected in mass number ranging from 0 to 250. $C_{32}N_8H_{18}$ ion was detected around the mass number of 505. finally, the $C_{32}N_8H_{18}$ ion beam extracted by mass spectrometry magnet was accelerated at the energy of 281 keV and implanted into the sample.

The NV centers created by $C_{32}N_8H_{18}$ ion implantation were observed using confocal fluorescence microscopy (CFM). The measurement of photon counts and optically detected magnetic resonance (ODMR) were performed with 532 nm laser and microwaves. FIG. 2(a) shows a typical image observed by a CFM with area of 20×20 μm^2. Isolated spots are clearly found from $C_{32}N_8H_{18}$ implanted region. FIG. 2(b) shows the ODMR spectra of the spot indicated by the circles and pentagon in FIG. 2(a). It is clear from the spectra that the spots labeled NV_A, NV_B, NV_C, and NV_D contain a single NV center with different axes. The spectrum labeled NV_{ABCD} is the result of the ODMR measurement of the spot indicated by the pentagon symbol in FIG. 1(a). from the number of dips in this spectrum, the creation of four NV centers with different orientation axes was observed per spot.

Therefore, we succeeded to create four NV centers in a spot by $C_{32}N_8H_{18}$ ion implantation. In the presentation, I will report on the probability of the creation of multiple NV centers.

Reference

[1] I. Jakobi, *et al.*, *J. Phys.*, **752**, 012001 (2016).

[2] T. Yamamoto, *et al.*, *Phys. Rev. B*, **88**, 201201 (2014).

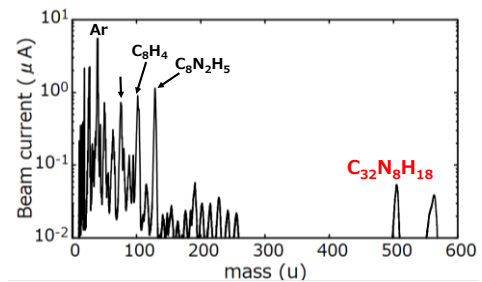[3] M. Haruyama, *et al.*, *Nat. Commun.*, **10**, 2664 (2019).

Acknowledgement
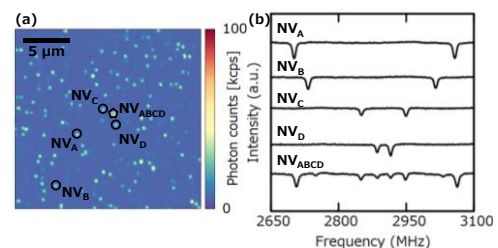
FIG. 1. Mass spectra from the $C_{32}N_8H_{18}$ ion source.

FIG. 2. (a) Typical CFM image (20×20 μm^2). (b) The ODMR spectra of the single NV centers and quadruple NV center.

Fabrication of diamond protective film using microwave plasma CVD towards high-quality quantum emitters

K. Hirokawa[1], K. Fukuda[1], P. Wang[1], T. Taniguchi[2], M. Hatano[1] and T. Iwasaki[1]

[1]*Department of Electrical and Electronics Engineering, School of Engineering, Tokyo Institute of Technology*

[2]*International Center for Materials Nanoarchitectonics, National Institute for Materials Science,*

hirokawa.k.ab@m.titech.ac.jp

Introduction

Quantum networks are expected to realize secure communication by using the transfer of quantum states. Quantum emitters which can generate a quantum entanglement state are necessary to construct quantum networks. Group-IV color centers in diamond has attracted due to the sharp zero photon line (ZPL) and resistance to external electric noise. Among the group-IV color centers, SnV and PbV are expected to have a long spin coherence time in the milli-seconds at Kelvin temperatures [1,2]. However, the fabrication process includes high-temperature anneal at 2100℃, resulting in deterioration of the sample surface, which frequently etches the incorporated color centers and hinders the fabrication of nanophotonic structures. To overcome this issue, in this study, diamond films were deposited on a diamond substrate containing SnV centers to protect during the high- temperature anneal.

Method and Results

Figure 1 illustrates the fabrication process. We used a IIa-type diamond substrate (Element Six). Sn ions were implanted into the substrate with an acceleration energy of 700 keV and a dose of $2 \times 10^9/cm^2$. Then, diamond films were deposited by two microwave plasma CVD systems for 40 hours in total. At the first growth stage, diamond films with low impurity concentrations were synthesized at the low growth rate. Then, at the next stage, thicker diamond films were grown using a high-power plasma CVD system. This sample was treated at 2100℃ under 7.7 GPa to form SnV centers in the IIa-type diamond substrate. Confocal fluorescence microscope observations were carried out at a cryogenic temperature.

The CVD film remained on the substrate after anneal at 2100℃. Figure 2 shows ZPL from the SnV centers after the high-temperature anneal. The two lines correspond to C- and D-peaks, originating from split energy levels of the SnV centers. These observations indicate that the deposited diamond films worked as a protective layer to form SnV centers.
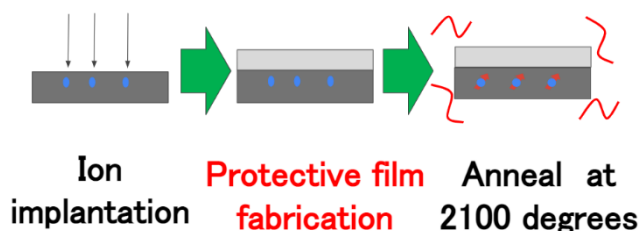

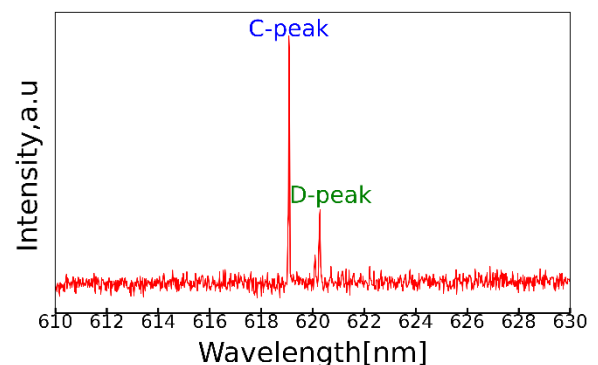FIG.1. Schematic diagram of protective film fabrication for the SnV center formation.

FIG.2. PL spectrum of SnV

Reference

[1]T.iwasaki et al, Phys. Rev. Lett, 119, 253601 (2017)

[2]P.Wang et al, ACS photonics,2947,2954(2021)

Acknowledgments

A compact quantum sensor head with side excitation of CVD diamond

Yuki Nishio[1], Yuji Hatano[1], Jaewon Shin[2], Daisuke Nishitani[1], Ryo Matsuki[1], Hiromitsu Kato[3], Shinobu Onoda[4],

Takeshi Oshima[4], Keigo Arai[1], Mutsuko Hatano[1], and Takayuki Iwasaki[1]

[1]*Department of Electrical and Electronics Engineering, School of Engineering, Tokyo Institute of Technology*

[2]*Yazaki Corporation*

[3]*National Institute of Advanced Industrial Science and Technology*

[4]*National Institutes for Quantum Science and Technology*

nishio.y.ac@m.titech.ac.jp

Introduction

A compact sensor system is important for practical applications of quantum diamond sensors using NV centers. There have been reports on nanotesla to sub-nanotesla sensitivities for the small modular diamond sensor, such as 3 $nT/\sqrt{Hz}$ by side excitation on a (100 crystal[1], 310 $pT/\sqrt{Hz}$ by perpendicular excitation on a (100 crystal[2], and 344 $pT/\sqrt{Hz}$ by perpendicular excitation on a (111 crystal[3]. In this report, we investigate the side excitation of a CVD diamond layer on a (111 crystal including a large volume of NV centers.

Method

The configuration of the sensor head fabricated in this experiment is shown in FIG.1. A 110 μm-thick ^{12}C-enriched CVD film grow n on 2.0✕ 2.0✕ 0.3 mm^3 IIa (111)substrate was used as the diamond sensor. The NV centers were formed by 5.0×10^{17} cm Ē B irradiation and high-temperature anneal. The excitation green laser was introduced on a sidewall of the CVD film, and the fluorescence emitted from the NV centers was then collected by a CPC lens and led into a photodiode through LPFs. The microwave antenna was made of copper tape and the microwave magnetic field was applied horizontally. The antenna was placed on an AlN heatsink plate. In order to excite only the NV-rich region in the diamond sample, the laser diameter was adjusted using a beam expander and focusing lens. A part of the excitation laser was extracted as a reference light to cancel the laser noise from the fluorescence. The optical system was placed in a 1 mm-thick permalloy single layer magnetic shielded box.

Result

First, we investigated the magnetically insensitive noise and slope of the lock-in ODMR by varying the deviation frequency (Fig. 2a. Although the slope takes the maximum value at a deviation frequency of 500 kHz, in this experiment, we set the deviation frequency around 350 kHz, where the noise/slope becomes small. The measured magnetic field noise spectrum is shown in Fig. 2b. The sensitivity was estimated to be 770 $pT/\sqrt{Hz}$ and the noise floor was 400 $pT/\sqrt{Hz}$ between 30-100 Hz. In this frequency range, the noise floor of magnetically sensitive is comparable to that of the magnetically insensitive. The shot-noise limit sensitivity, calculated from the contrast and linewidth measured from the ODMR, is 15 $pT/\sqrt{Hz}$, expecting a higher magnetic field sensitivity by improving the measurement system. This work was supported by MEXT Q-LEAP Grant Number JPMXS0118067395.

Reference

[1]J. Webb et al., Appl. Phys. Lett. 114, 231103 (2019) [2]R. Patel et al., Phys. Rev. Appl. 14, 044058 (2020)
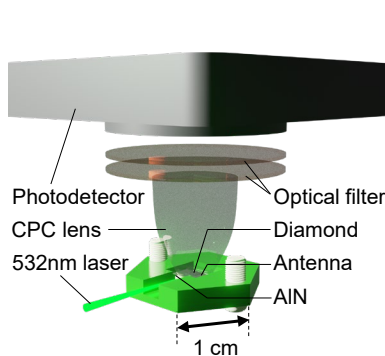[3]F. Stürner et al., Adv. Quantum Technol. 4, 2000111 (2021)

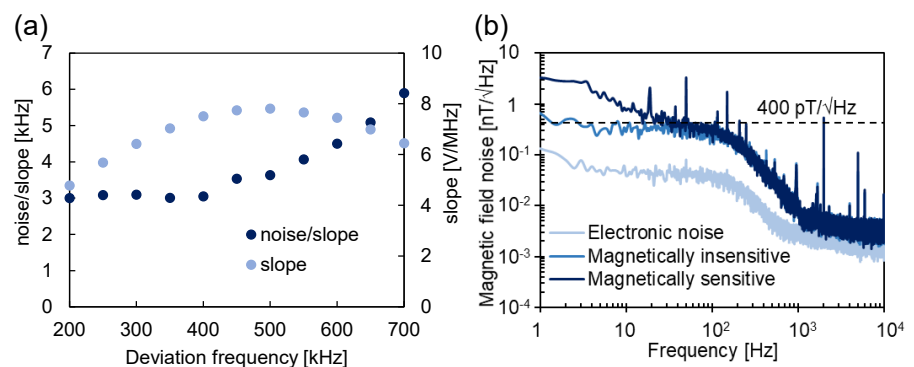FIG.1 Sensor module for side laser excitation.

FIG.2 (a) Ratio of the magnetically insensitive noise to the slope of the lock-in ODMR and the slope depending on the deviation frequency. (b) Measured FFT spectrum of sensitivity. The black dotted line indicates 400 $pT/\sqrt{Hz}$.

Hybrid integration of Si₃N₄ grating structure on diamond NV substrate for efficient photon extraction

Ryota Katsumi[1, 2], Takeshi Hizawa[1], Akihiro Kuwahata[2, 3], Takayuki Iwasaki [4], Mutsuko Hatano [4],

Fedor Jelezko[5], Masaki Sekino[2], and Takashi Yatsui[1, 2]

[1] *Graduate School of Engineering, Toyohashi University of Technology*

[2]*Graduate School of Engineering, The University of Tokyo*

[3]*Graduate School of Engineering, Tohoku University*

[4] *School of Engineering, Tokyo Institute of Technology*

[5]*Institute of Quantum Optics, Ulm University*

katsumi.ryota.ti@tut.jp

Introduction

Nitrogen-vacancy (NV) centers in diamond is a promising candidate for a quantum sensor, especially a sensitive magnetometer thanks to their excellent spin property[1,2]. However, their demonstrated magnetic field sensitivity is far beyond those based on superconducting quantum-interference devices. One of the critical issues is the low extraction efficiency of the emitted photons from the diamond NV substrate[3]. This can be overcome by implementing the nanostructure on diamond including gratings, but the fabrication of such structure on diamond is technically difficult.

Method

In this work, we demonstrate the hybrid integration of grating structure on a diamond NV substrate using transfer printing, which is based on a simple pick-and-place operation[4]. Figure 1(a) displays the SEM image of the grating based on Si₃N₄, which is transparent for the NV emission wavelength of around 700 nm. To pick them up, we employed the air-bridged structure for the grating. By using the transfer printing [Fig. 1(b)], the Si₃N₄ grating was integrated on the diamond NV substrate. Figure 1(c) displays the optical microscope image of the fabricated device. The grating is indeed bonded with the diamond NV substrate. The detailed design and characterization will be discussed in the presentation.
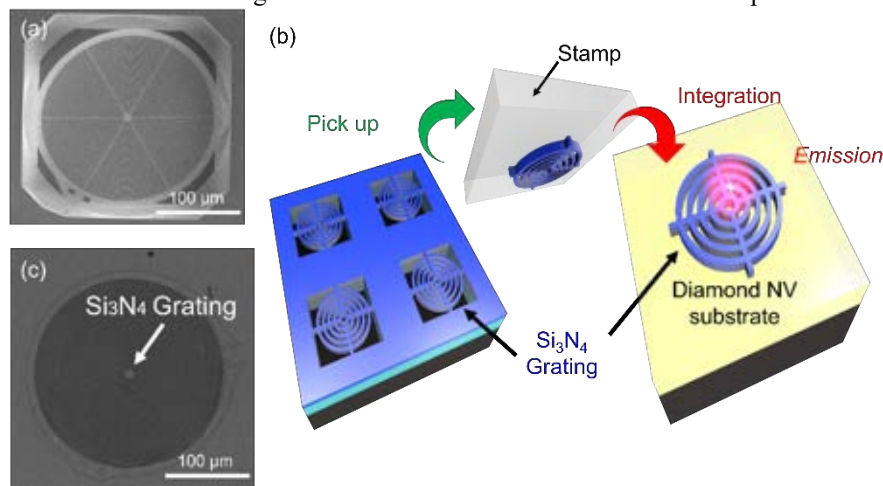

FIG. 1. (a) SEM image of the fabricated Si₃N₄ grating. (b) Schematics of the transfer printing-based integration of Si₃N₄ grating on diamond. (c) Optical microscope image of the fabricated device.

Acknowledgement

References

[1]   J. M. Taylor, *et al.,* Nat. Phys. **4**, 810 (2008).

[2]   A. Kuwahata, *et al.,* Sci Rep **10**, 2483 (2020).

[3]   D. Le Sage, *et al.,* Physical Review B **85**, 121202 (2012).

[4]   R. Katsumi, *et al.,* Optica **5**, 691 (2018).

SE-03A-γ2-01

Superconducting nanostrip single-photon detectors with dielectric multilayer cavities

Fumihiro China[1], Shigehito Miki[1,2], Satoru Mima[1], Masahiro Yabuno[1], Shigeyuki Miyajima[1] and Hirotaka Terai[1]

[1] *Advanced ICR Research Institute, National Institute of Information and Communications Technology*

[2]*Graduate School of Engineering, Kobe University*

f-china@nict.go.jp

Introduction

Superconducting nanostrip single-photon detectors (SNSPDs) have attractive features such as high detection efficiency, low dark count rate, and low timing jitter, and are promising instruments in various fields, including quantum information science [1]. The superconducting nanostrip consisting of a thin and narrow meandering line potentially has photon sensitivity in a wide wavelength range from ultraviolet to mid-infrared, but the optical absorptance of only a single nanostrip layer is as low as few tens of percent. The SNSPDs integrated with dielectric multilayer (DML) cavities, as shown in FIG. 1, are effective structures to enhance the optical absorptance of the nanostrips at the target wavelengths. The DMLs are composed of two dielectric materials with different refractive indexes. By optimizing the layer structure such as the number of layers and film thickness of each layer, the optical properties of SNSPDs can be designed flexibly according to the requirement [2]. In this presentation, we show the development of SNSPDs with DMLs for various wavelength regions.

Method

We have designed and developed SNSPDs with DMLs using SiO_2 and TiO_2 for the visible wavelength, SiO_2 and Si for the telecom wavelength, and Ta_2O_5 and Si for the mid-infrared region, respectively. FIG. 1 shows a schematic of an SNSPD with a DML composed of SiO_2 and TiO_2, which is designed for 780 nm wavelength region. First, the layer structure of the DML was optimized for the target wavelength using a thin film calculation software. Subsequently, we simulated the absorptance dependence on the polarization state of incident photons by finite-element analysis. As results, the optimized number of layers and the total thickness of the DML are 17 layers and 2.02 μm, respectively. Since it was also confirmed that the optical absorptance of the nanostrip depends on the polarization state of the incident photon, SiO film is deposited on the nanostrip to minimize the polarization sensitivity at the wavelength of 780 nm. Then, we fabricated the nanostrip devices according to the optimized design of SNSPD with the DML and evaluated the wavelength dependence of the system detection efficiency (DE) using a supercontinuum light source. FIG. 2 shows the wavelength dependence of the optical absorptance and measured system DE. The obtained dependence of the system DE well agrees with optical absorptance dependence in the simulations, and we obtained a high system DE of 85% at 780 nm. The developments of SNSPDs for other wavelengths will be talked in the presentation.

Acknowledgment

Reference

[1]R. H. Hadfield, *Nat. Photon.*, 3, 696–705 (2009).

[2]T. Yamashita, K. Waki, S. Miki, R. A. Kirkwood, R. H. Hadfield, H. Terai, *Sci rep.*, 6, 35240 (2016).
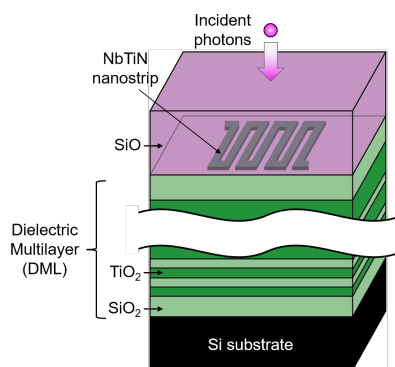
FIG. 1. Schematic of the device structure of an SNSPD with a DML. The number of layers and total thickness of the DML are 17 layers and 2.02 μm, respectively.
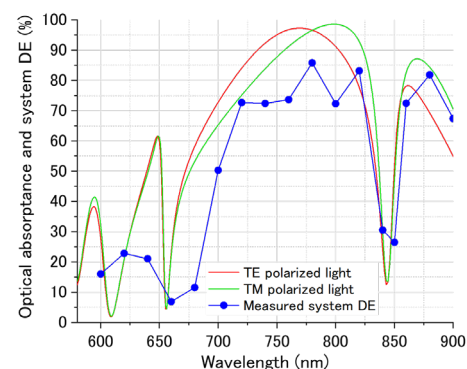

FIG. 2. Comparison of the simulated optical absorptance of the NbTiN nanostrip and the measured system DEs.

Estimation of the quantum efficiency of the up-conversion system based on injection-locked dual oscillators

Masayuki Hojo[1], Shuntaro Tani[2], Yohei Kobayashi[2], and Koichiro Tanaka[1]

[1]Department of Physics, School of Science, Kyoto University

[2]ISSP, The University of Tokyo

hojo.masayuki.33e@st.kyoto-u.ac.jp

Introduction

Spontaneous parametric down-conversion (SPDC) is essential tool for a quantum light source in the infrared region ranging 2-5 μm for the purpose of material identification, chemical analysis, and gas sensing. However, SPDC process has a technical limitation of low efficiency and can be detected only by sensitive detectors. Up-conversion detecting system has been demonstrated to bridge such a gap. So far, existing technique[1] has been concentrated into the conversion efficiency, in which the temporal duration of the light source was highly broad. In this work, we implement the up-conversion detector using two Er- and Yb-doped fiber lasers (EDFL and YDFL) with the duration narrower than the conventional one.

Method

Figure 1 illustrates the schematics of the up-conversion system. The EDFL output at 1.56 μm was split into two ports, which served as the injecting seed and the pump for down frequency generation (DFG) process in PPSLT, respectively. The repetitions of EDFL and YDFL was synchronized at 57.9 MHz. The YDFL output had the spectral shape narrowed by Fiber-Bragg-Grating (FBG) and was boosted to 100mW. Similarly, the amplified pulse was divided into two portions, the DFG port and the up-conversion port. In the DFG port, the two pulses at 1.03 and 1.56 μm were spatially combined with a wavelength division multiplexer (WDM) and produced a MIR pulse by DFG process. The MIR light source was then introduced into PPLN crystal. The pump for the up-conversion was focused into PPLN in the collinear configuration with the MIR pulse. The SFG signal in the visible region was detected by a sensitive detector.

In our presentation, we will report the result of up-conversion detection and discuss about the system improvement.
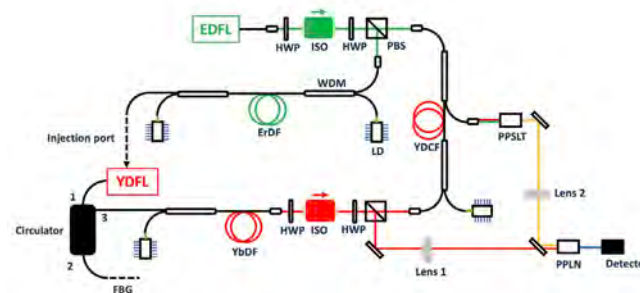

Fig. 1 Schematics of the whole system.

Reference
1.   Huang, K. *et al. Photonics Res.* **9**, 259 (2021).

4th IFQMS

QUANTUM
INNOVATION
2021

Selective measurement of biexciton luminescence by photon correlation spectroscopy

Hiroya Seki[1], Keita Hashimoto[2], Jun Ishihara[2], Kensuke Miyajima[2], Ryosuke Shimizu[1]

[1]Department of Engineering Science, The University of Electro-Communications

[2]Department of Applied Physics, Tokyo University of science

s2043006@edu.cc.uec.ac.jp

Introduction

Coincidence measurement performed by two detectors is a common technique to detect photon pairs in quantum optical experiments [1] and allows us to extract two-photon events from the input state of light [2]. This technique has been used in demonstrating fundamental concepts of quantum mechanics, quantum information protocols, and quantum imaging. On the other hand, we also expect the application of coincidence measurement to spectroscopy as a new development of quantum technology. Combining the coincidence counting with frequency-resolved measurement could bring us a new approach to spectroscopy in a quantum manner. Hereafter we refer to it as photon correlation spectroscopy (PCS) [3]. The Photon-number-resolving ability of PCS may provide a powerful tool to analyze a complex quantum system in condensed matter. Here we present a proof-of-concept experiment of PCS with biexciton luminescence.

Method

Biexciton is generated via a two-photon resonant excitation by the second harmonic of a mode-locked Ti: sapphire laser, and then decays into two polaritons; a higher energy polariton (HEP) and a lower energy polariton (LEP). After propagating in the crystal, the polaritons are converted into photons at the crystal surface. In this process, the sum of the two-photon energy should be the same as biexciton energy due to the phase-matching condition. We employed a femtosecond laser with the bandwidth of 4.4 nm, corresponding energy width of 9.0 eV, to clarify the photon-number-resolving ability. In this situation, the spectrum of Rayleigh scattering light of the laser overlaps that of biexciton luminescence. Therefore, it is difficult to distinguish the biexciton luminescence from the laser spectrum. In contrast, PCS enables us to observe HEP and LEP due to the photon-number-resolving ability.

In order to characterize two-photon spectral distributions, joint spectral intensity (JSI) plotted in a two-dimensional space has been employed in the quantum optics field [4]. The JSI represents the two-photon probability distribution as a function of the energy of the constituent photon. Experimentally, we recorded the coincidence counting values by scanning the transmission frequency of two monochromaters for the JSI measurement.

Figure 1 shows the measured JSI of biexciton luminescence. We can see a single peak distribution caused by coincidence counts of HEP and LEP. We estimated the spectral width of HEP (LEP) as 0.94 (1.2) meV from the projection of the JSI onto the vertical (horizontal) axis, which is narrower than the bandwidth of the laser. This result implies a successful demonstration of PCS.
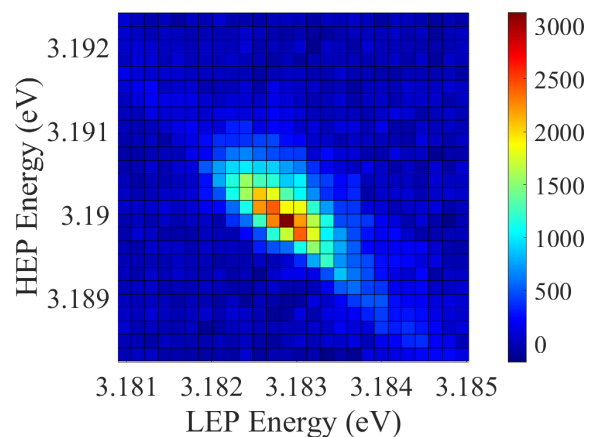

FIG. 1. JSI of biexciton luminescence.

Reference

[1] C. K. Hong, Z. Y. Ou, and L. Mandel, *Phys. Rev. Lett.*, **59**, 2044-2046 (1987).

[2] H. Seki, K. Miyajima, R. Shimizu, arXiv:2109.03715 (2021)

[3] C. M. Muñoz, and F. Schlawin, *Phys. Rev. Lett.*, **124**, 203601 (2020).

[4] P. G. Evans, R. S. Bennink, W. P. Grice, and T. S. Humble, *Phys. Rev. Lett.*, **105**, 25361 (2010).

Towards Optical Manipulation of Gold-Nanoparticles for Efficient Single Photon Sources

Rui Sun[1], Yining Xuan[1], Soyoung Baek[1], and Keiichi Edamatsu[1]

[1]*Research Institute of Electrical Communication, Tohoku University*

sun@quantum.riec.tohoku.ac.jp

Quantum dot is a promising candidate for constructing a single photon source because of its broad and continuous excitation spectrum, adjustable wavelength, high photochemical stability, and long fluorescence lifetime[1]. Our research focuses on the single photon source based on quantum-dot-gold-nanoparticle coupled system on optical nanofiber[2]. Combining with the Purcell effect[3], the rise time of the second order intensity correlation function for quantum dot can be enhanced. However, the position of gold-nanosphere on nanofiber is entirely random, which makes the quantitative study of single-photon emission rate difficult. We propose a non-contact method to control the position of a gold-nanoparticle on the nanofiber making use of an optical tweezer. We calculate the optical responses and heating effects of a gold-nanoparticle trapped in optical tweezer to define the optimal wavelength and laser power for the experiment.

The optical response of a gold-nanoparticle submerged in water and trapped in an optical tweezer is calculated based on Mie theory. Figure 1 is the scattering and absorption efficiencies of a gold-nanoparticle in an optical tweezer. The red and blue curves are the scattering (Q_{sca}) and absorption (Q_{abs}) factors, respectively. The abscissa is the size parameter (ka) of the gold-nanoparticle; k is the wave number of the light and a is the radius of gold-nanosphere. Here, the gold-nanoparticle size ranges from 0 to 200 nm. For the same particle size, the longer the optical wavelength is, the weaker the effect of absorption and scattering.
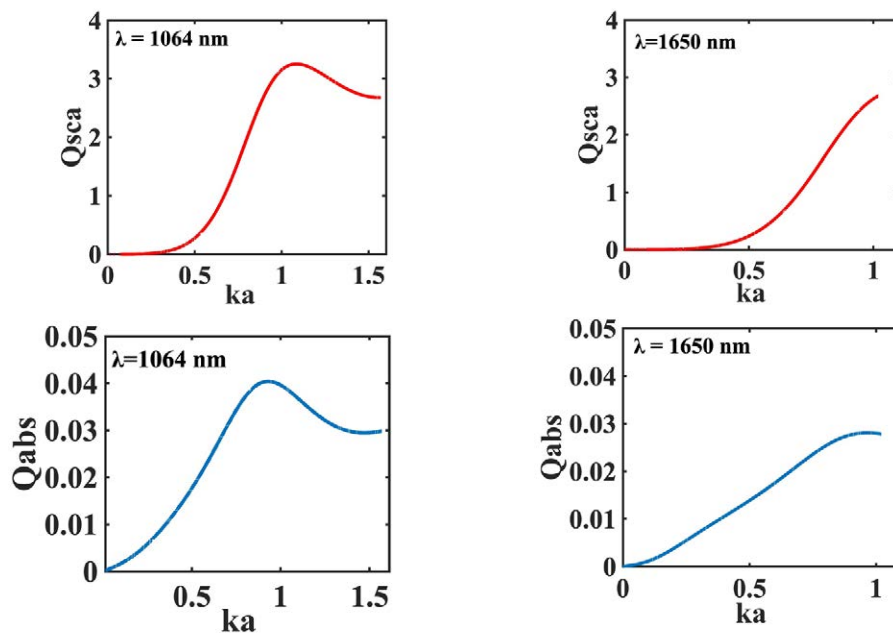
FIG. 1. Scattering and absorbing efficiencies of gold-nanoparticle trapped in optical tweezer.

References

[1] O. Gazzano and G. Solomon, *J. Opt. Soc. Am. B*, 33, C160-C175 (2016).
[2] M. Sadgrove, M. Sugawara, Y. Mitsumori and K. Edamatsu, *Sci Rep, 7*, 17085 (2017).
[3] Q.Gu, and Y. Fainman, *Semiconductor Nanolasers,* (pp. 65-90) (2017).

Single photon emission from a quantum-dot-gold-nanostar coupled system on an optical nanofiber

Yining Xuan[1], Masakazu Sugawara[1], Rui Sun[1], Soyoung Baek[1], Keiichi Edamatsu[1], and Mark Sadgrove[2]

[1]*Research Institute of Electrical Communication, Tohoku University*

[2]*Department of Physics, Faculty of Science, Tokyo University of Science*

xuan@quantum.riec.tohoku.ac.jp

Single-photon emitters play an important role in many leading quantum technologies such as quantum communications and quantum cryptography. Therefore, coupling them to existing fiber network can be a promising candidate for the various applications in quantum network. As a carrier of photon transportation, optical nanofiber has the advantage of ultra-low loss, low cost and high coupling efficiency [1]. Since the nanofiber has a diameter of hundreds of nanometers, photons emitted from single photon emitters can be coupled into nanofiber through the evanescent field directly. Therefore, single-photon source's effective incorporation into nanofibers shows great potential in the construction of fiber-based quantum information network. In 2012, Yalla *et al.* demonstrated the coupling of single photons from quantum dots into the nanofiber [2]. After that, Liebermeister *et al.* succeed in coupling single photons from color centers in a diamond into the nanofiber [3]. Nevertheless, how much we can improve the coupling between the single-photon emitters and the nanofiber is still an open question that needs to be addressed. In this research, in order to achieve Purcell-enhanced single-photon emission from a quantum dot (QD, we place gold nanoparticles, especially gold nanostars (GNS, in the vicinity of the quantum dot located on the surface of an optical nanofiber. By measuring the rise time of the second order correlation function $g^{(2)}(\tau)$ for both the GNS-QD system and the sole QD system, Purcell-enhancement can be verified.

We fabricate a nanofiber with the diameter of 474 nm by heating-stretch method [4][5], and place a GNS and a QD on the surface of a nanofiber. Figure 1 shows scanning electron microscope (SEM image of GNS-QD coupled system. By scanning a laser beam spot along the nanofiber axis and measuring the photoluminescence (PL signal from the QD and the scattered light from the GNS, we confirm the GNS and the QD is located within 1.5 μm interval. Next, we measure second order correlation function $g^{(2)}(\tau)$ for both the GNS-QD system and the sole QD system on the same nanofiber. See Figure 2. The obtained $g^{(2)}(0)$ for the GNS-QD and Sole QD was less than 0.5, a signature of anti-bunched single photons. The rise time of $g^{(2)}(\tau)$ for the GNS-QD and the SQD are obtained to be 167 ns and 107 ns, respectively; the GNS-QD exhibited ~36 % reduction of the rise time in comparison to the SQD. Although it is likely to originate from Purcell enhancement, more detailed and complete measurement and analysis are necessary to conclude.
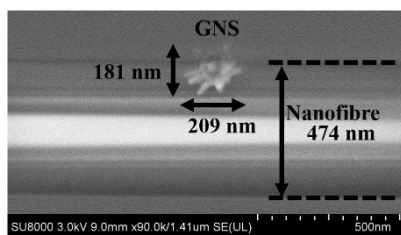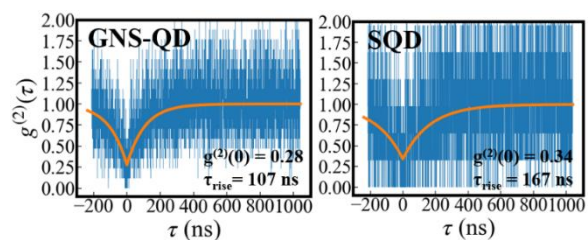
FIG. 1. SEM image of GNS-QD coupled system.

FIG. 2. $g^{(2)}(\tau)$ measurement of GNS-QD coupled system and sole QD system, respectively.

Reference

[1]M. Sadgrove, M. Sugawara, Y. Mitsumori, and K. Edamatsu, *Sci. Rep.*, 7, 17085 (2017).
[2]R. Yalla, K. Nayak, and K. Hakuta, *Opt. Express*, Vol. 20, Issue 3, 2932 (2012).
[3]L. Liebermeister et al., *Appl. Phys. Lett.*, 104, 031101 (2014).
[4]M. Sugawara, Y. Mitsumori, K. Edamatsu, and M. Sadgrove, *Opt. Express*, 28, 18938 (2020).
[5]M. Sadgrove, T. Yoshino, M. Sugawara, Y. Mitsumori, and K. Edamatsu, *Phys. Rev. Applied*, 16, 044034 (2021).

SE-03A-γ2-06

Focusing constraints on coupling efficiency of collinear type-I degenerated SPDC photon pairs into a single-mode fiber

Nicolas Schwaller[1,2], Geobae Park[1], Ryo Okamoto[1,3], and Shigeki Takeuchi[1]

[1]*Department of Electronic Science and Engineering, Kyoto University*

[2]*Institute of Physics, Swiss Federal Institute of Technology Lausanne (EPFL), Lausanne, Switzerland*

[3]*Japan Science and Technology Agency, PRESTO*

schwaller.nicolas.52z@st.kyoto-u.ac.jp

Introduction

Entangled photon pairs represent an essential resource for various quantum technologies, such as quantum key distribution, quantum computing or quantum imaging. A common process to produce correlated pairs is spontaneous parametric downconversion (SPDC) of pump photons into pairs of entangled photons which are then coupled into a single-mode (SM) fiber. For most applications, it is desirable to maximize the coupling efficiency of the entangled pairs into the SM fiber, as well as the rate of pairs that can be collected. Systematic studies about the maximization of these quantities have been carried out for specific parameters of SPDC, e.g. using type-II phase-matching condition [1]. However, despite advances on theoretical modelling [2,3], other SPDC configurations still lack experimental evidence to confirm the dependence of the coupling efficiency on the main parameters of the setup. This study focuses on collinear degenerated co-polarized SPDC photon pairs. They are relevant for various applications such as single mode squeezed states for gaussian boson sampling, and non-linear interferometers.

Method

We investigate the dependence of the correlated-mode coupling efficiency η_c on pump and collection beam waists by continuously varying their size thanks to two beam expanders (FIG. 1). We generate type-I SPDC by pumping a bulk beta barium borate (BBO) crystal of $L= 3$ mm length with a continuous wave (CW) 404 nm laser. We measure the coupling efficiency using coincident detections from single photon counting modules (SPCMs), and study the impact of different focusing conditions of the pump and collection beam. The estimated coupling efficiency was obtained by considering the losses of the optics and the experimentally determined quantum efficiencies of the SPCMs. The observed η_c reached up to 98%.
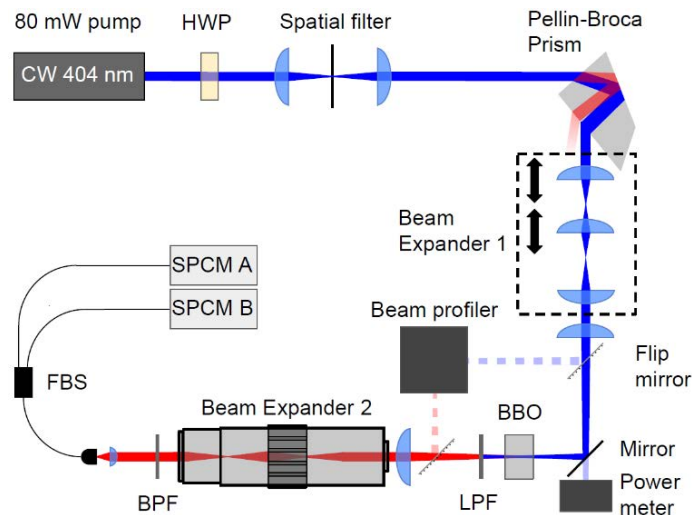

FIG. 1: Experimental setup enabling to change the focus of pump and collection beam in the crystal.

Reference

[1]P. Ben Dixon *et al.*, *Phys. Rev. A*, 90(4), 1-9 (2014).
[2]R. S. Bennink, R. S., *Phys. Rev. A*, 81(5), 1–10 (2010).
[3]H. E. Guilbert *et al.*, *IEEE Journal of Selected Topics in Quantum Electronics,* 21(3), 215-224 (2015).

SE-04-01

Quantum sensing enabled by spin qubits in diamond

Fedor Jelezko

Institute of Quantum Optics, Ulm University

Abstract

Single nitrogen vacancy (NV) color centers in diamond currently have sufficient sensitivity for detecting single external nuclear spins and resolve their position within a few angstroms. The ability to bring the sensor close to biomolecules by implantation of single NV centers and attachment of proteins to the surface of diamond enabled the first proof of principle demonstration of proteins labeled by paramagnetic markers and label-free detection of the signal from a single protein. Single-molecule nuclear magnetic resonance (NMR) experiments open the way towards unraveling dynamics and structure of single biomolecules. However, for that purpose, NV magnetometers must reach performance comparable to that of conventional solution state NMR. We will discuss new techniques allowing to combine high spectral resolution and sensitivity in nanoscale NMR. The ability to sense nuclear spins by NV centers also enables the transfer of polarization from optically polarized spins of NV centers to external nuclear spins. Such diamond based techniques for dynamic nuclear spin polarization are very promising for the enhancement of sensitivity of conventional MRI imaging.

Programmable quantum simulators based on spins in diamond

Tim Taminiau

QuTech and Kavli Institute of Nanoscience, Delft University of Technology, the Netherlands

Abstract

Spins associated to optically active defects in diamond provide a versatile platform for quantum science and technology. In this talk, I will discuss our recent advances in realizing programmable quantum simulators based on individually controllable carbon-13 nuclear spins in diamond. I will present how one can use a single nitrogen-vacancy (NV) centre to sense, characterize and control a large number of spins in its environment [1,2,3]. By controlling the interactions between the spins it becomes possible to create a variety of many-body Hamiltonians with tunable parameters. As an example, I will discuss our investigation of a discrete-time crystal stabilized by many-body localization, a new out-of-equilibrium phase of matter [4].

[1] M. H. Abobeih et al., Nature 576, 411 (2019)
[2] C. E. Bradley et al., Phys. Rev. X. 9, 031045 (2019)
[3] M. J. Degen et al., Nature Commun. 12, 3470, 2021 (2021)
[4] J. Randall et al., arXiv:2107.00736 (2021)

SE-04-03

Development and optimisation of diamond for quantum technologies

Matthew Markham

Element Six

Abstract

Quantum technologies is attracting significant investment due to the range of potential applications, but behind any new technology are the enabling materials. Diamond is one such material and ensembles of negatively-charged nitrogen-vacancy (NV-) centres constitutes a promising platform for sensing applications utilizing the quantum properties of this defect. However, the sensitivity of present NV-ensemble devices and the need for diamond material with reproducible properties has the potential to hinder progress toward many envisioned commercial-scale applications. The work covered in this presentation will address the material-related challenges associated with the development of diamond materials with reproducible properties for diamond quantum technologies.